Fall 2018

Developing a methodology for estimating the growth of radiated emission from multi-modular systems

Kaustav Ghosh

Department:

DEVELOPING A METHODOLOGY FOR ESTIMATING THE GROWTH OF RADIATED EMISSION FROM MULTI-MODULAR SYSTEMS

by

KAUSTAV GHOSH

A THESIS

Presented to the Faculty of the Graduate School of the

MISSOURI UNIVERSITY OF SCIENCE AND TECHNOLOGY

In Partial Fulfillment of the Requirements for the Degree

MASTER OF SCIENCE IN ELECTRICAL ENGINEERING

2018

Approved by

Dr. David J. Pommerenke, Advisor
Dr. Victor Khilkevich
Dr. Jun Fan

ABSTRACT

The large multiscale problems are commonly faced in real-world applications such as analysis of electromagnetic interference for a printed circuit board installed on a large platform with connected cables, wires and other high speed interfaces. EMI problems are not uncommon in high speed systems which involve multiple modules of complex hardware. As the system clock frequency and data rate increases, so does the challenges in controlling the EMI in such systems. The costs to prototype and to develop networking equipment are growing as a result of increasing complexities and densities. EMC regulations require radiated emission testing to be done in a worst-case condition that typically requires a fully loaded system. Typical networking equipment holds tens of nearly identical line cards and hundreds of optical modules within them. Thus, if a path to study the growth of electromagnetic (EM) radiation from these systems using less hardware is adopted, development costs can be significantly reduced. Due to the complexity of the system, prediction of the maximum radiated field strength cannot be exact. However, an estimation of emission growth with number of radiators is possible through statistical analysis. This thesis presents a methodology and the considerations (frequency/phase behavior, radiation pattern, directivity, and their possible variations) to account for approximating the maximal E-field. This allows us to predict the growth pattern of emission as modules are added into a system, and the input parameters for the statistical simulation. The method developed in this study can be used for any multi-modular systems provided all the key parameters are taken into consideration correctly.

ACKNOWLEDGMENTS

I would like to express my gratitude to all those who have helped me during this research. Firstly, I would like to thank my advisor Dr. David Pommerenke for giving me the opportunity to work on this project, his valuable insights and suggestions have helped me to overcome many hurdles during this work. I am grateful to him for the advice and guidance he gave me throughout my Master's program. I also thank Dr. Pommerenke for his moral support during my tough times by understanding and encouraging me to focus on my goals. I would like to thank Dr. Victor and Dr. Fan for being part of my thesis committee and taking time to review this work. I would like to thank Abhishek Patnaik (Ph.D. student) for his continuous mentoring and guidance, Javad Meiguni and Wei Zhang at Missouri University of Science and Technology for their contribution towards this work. I thank Philippe Sochoux and Jacques Rollin from Juniper Networks for their valuable guidance and immense support during the course of this study and also for providing the hardware which served as a research subject.

A special thanks to all my friends whose constant support and encouragement has always been crucial for me. Finally, I would like to dedicate this work to my parents (Chaitali and Pijush Ghosh) for their emotional support and unconditional love and sacrifices.

TABLE OF CONTENTS

Page

LIST OF ILLUSTRATIONS

Page

LIST OF TABLES

1. INTRODUCTION

Testing emissions from large systems poses challenges with the selection of the configurations as testing cannot cover every permutation of EUT configurations. EMC regulations require radiated emission testing of equipment to be performed in a configuration as close as possible to the actual installation for worst-case emissions. Electronic equipment should be regarded as unintentional radiators unless defined in their functionality, which means the direction corresponding to the maximum emission is not known by the design.

The maximum emission from an unintentional radiator cannot be known prior to a complete 3D radiation pattern measurement, which is time-consuming. To find a maximum from such unintentional radiators, it would be necessary to determine the directivity of the radiating element. In earlier work, stochastic approaches were derived to describe the probability distribution of the directivity of such systems [1, 2]. Other work [3] deals with the maximum directivity based on electrical size of the device defined as $k \cdot a$, where k is the wavenumber and 'a' is the radius of minimum sphere enclosing the device. All these estimations have either over- or underestimated the directivity for electrically large equipment under test (EUT) [4]. Another disadvantage of traditional measurement methods is to miss the E_{Max}. This happens if the radiating elements have a very narrow beam and propagate in directions not covered by the scan area. Total radiated power (TRP) measurement in a reverberation chamber is an alternative to the traditional method, especially at frequencies above 1 GHz [5, 6]. The directivity of the EUT has to be known in advance in order to convert the measured radiated power into a comparable maximum field strength of standard emission measurements. Measurements

of TRP, combined with directivity, can be used to predict the maximum radiated field from an unintentional source above 1 GHz [7].

Traditional testing of radiated emissions from larger systems with multiple identical modules are expensive and time-consuming. CISPR 22, CISPR 32, and FCC part 15 (ANSI C63.4) propose a 2 dB rule when dealing with multi-modular systems. The worst-case quantity to test radiated emissions is reached when the addition of the same type of multiple module produces an increase of less than 2 dB in emission while complying within the limits. Studies in [8] have observed a saturation of emission when testing incremental quantities of identical units as shown in Figure 1.1.

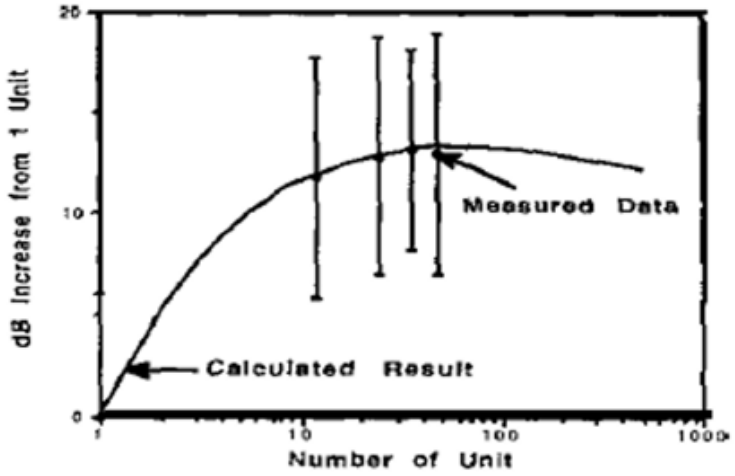

Figure 1.1. Results from [8] showing the saturation of radiated emission from addition of identical units in a system.

In this article, a first step towards developing a methodology to estimate the growth of emission from systems hosting multiple nearly identical modules is taken. The prediction will estimate the emissions of the fully loaded system as measured by the

CISPR 22 standard, based on the data obtained with only a fraction of the hardware. In order to describe growth of emissions with increase in system loading, a form of extrapolation will be needed. This is achieved through statistical simulation, but first it is necessary to describe the electromagnetic characteristics for the individual elements comprising the system. There are trade-offs between the levels of analysis, input information available, and measurement uncertainties.

2. MOTIVATION

When good design practices are followed while developing high end network routers and network switches, but the end design still fails the EMC compliance, it involves lot of resources including human, monetary and infrastructure. This often leads to huge expense and loss of hours for industries who are in a cut-throat competition market. The cost to prototype these equipment and the hours spent in testing for compliance is increasing due to complexities and high speed which is an unfavorable situation for the industries. So, if we adopt a path to study the growth of EM radiation from fewer prototyped hardware, development costs can be significantly reduced. The main goal of this project is to develop a methodology which can estimate the final emission from a large system by testing fractional hardware. Having a good understanding of the factors that influence the growth of radiation will help develop a mathematical or statistical and experimental method that allows for the estimation of the maximal E-field from a fully loaded test setup using a few tests performed with less than fully loaded systems. The method should not only allow for the estimation of the maximal E-field for the fully loaded case, but it should provide the uncertainty of this estimate as well. Also, how the uncertainty of the estimate is affected by the number of tests performed with less than full loading and how the uncertainty depends on various factors such as instrument settings, frequency, phase, synchronization, polarization, etc. needs to be understood.

Better understanding of the relationship between total radiated power (TRP) and maximal E-field is very important for this study. In this case the maximal E-field is defined as the field seen in an EMC semi-anechoic chamber, which does not measure in

all directions of the radiation. If we can estimate the EMI scaling when multiple modules are connected to a large system, a calculated risk can be taken towards reducing the hardware expense in testing or in relaxing the requirement of adding additional hardware cost. In this way a limited amount of hardware can be used for EMI testing and then through statistical analysis, an estimate of the EUT emission amplitude seen in an EMC chamber for a fully loaded system can be determined.

3. BACKGROUND

3.1 ALTERNATE METHOD FOR EMISSION MEASUREMENT

Electric field strength is usually used to quantify the unwanted radiated emission of electronic equipment. These measurements are mostly performed in test sites with a perfectly conducting ground plane. The radiation pattern of a EUT becomes irregular at higher frequencies especially above 1 GHz when they are electrically large and hence doesn't ensure that the max field strength be measured in a test site like OATS or semi-anechoic chamber. Efficient alternative test methodologies or facilities are needed when extending the measurement frequency range beyond 1 GHz which also provides faster and much cheaper ways to test. Total radiated power measurement of EUT seems more plausible than dealing with E field strengths beyond 1 GHz and the mentioned alternative test sites facilitate this measurement. The TRP measured is used to estimate the maximum E field strength which might be very close to what we get from a standardized test site. Figure 3.1 illustrates a typical test site arrangement as defined in standards.

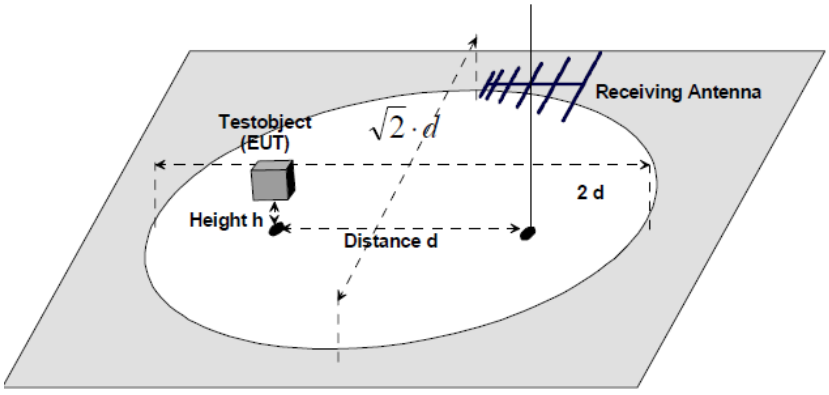

Figure 3.1. Test site as defined in standards [6]

According to IEC 61000-4-21, measuring the amount of power received by the antenna and correcting for the chamber losses can be used to determine the amount of RF power radiated by a device placed in a reverberation chamber (RVC). The power radiated from a device can be determined using either the average or maximum received power as:

$$P_{radiated} = \frac{(P_{avgreceived} \times \eta_{Tx})}{CVF} \quad (1)$$

$$P_{radiated} = \frac{(P_{Maxreceived} \times \eta_{Tx})}{CLF \times IL} \quad (2)$$

Where,

$P_{radiated}$	is the radiated power from the device (within measurement bandwidth)
CVF	is the chamber validation factor
CLF	is the chamber loading factor
IL	is the chamber insertion loss
$P_{avgreceived}$	is the received power(within measurement bandwidth) as measured by the reference antenna averaged over the number of tuner steps
$P_{Maxreceived}$	is the maximum power received (within the measurement bandwidth) over the number of tuner steps
η_{Tx}	is the antenna efficiency factor for the Tx antenna used in calibrating the chamber and can be assumed to be 0.75 for log periodic antenna and 0.9 for horn antenna.

The field strength generated by the EUT at a distance of *R* meter(s) at height *h* above perfectly conducting ground plane can be estimated from TRP measurement using the equation:

$$E_{Radiated} = g_{max}\sqrt{\left(\frac{D_{max} \times P_{radiated} \times \eta_0}{4\pi R^2}\right)} \quad (3)$$

Where,

$E_{radiated}$	is the estimated field strength generated by the EUT (V/m)
$P_{radiated}$	is the radiated power (averaged or max over tuner steps)
R	is the distance from the EUT at which we want to estimate the field strength. This shall be sufficient to ensure far field criteria at the frequency of interest.
η_0	is the intrinsic impedance of free space, approx. 377 Ω
D_{max}	is the maximum directivity of the EUT (dimensionless quantity)
g_{max}	is the dimensionless geometry factor accounting for ground plane reflections

This approach is mainly based on two parameters:

a) Geometrical factor

b) Directivity of EUT (D_{max})

3.2 GEOMETRICAL FACTOR

Geometrical factor g_{max} is accounting for the ground plane reflections in an OATS. g_{max} is a parameter of the test site configuration and the EUT has no effect on it. EUT emissions over a ground plane under far field condition needs to implement image theory and thus the worst case value can never be higher than twice the E field value of

free space. g_{max} also accounts for the height scan of the receiving antenna during the standard measurement in a site like OATS. g_{max} as per the Figure 3.2 is defined as:

$$g_{max} = \left\{ \left| \left(\frac{r}{r_1}\right) e^{-jkr_1} - \left(\frac{r}{r_2}\right) e^{-jkr_2} \right|_{max} \quad for\ horizontal\ polarization \right. \tag{4}$$

$$g_{max} = \left\{ \left| \left(\frac{s^2}{r_1^2}\right)\left(\frac{r}{r_1}\right) e^{-jkr_1} + \left(\frac{s^2}{r_2^2}\right)\left(\frac{r}{r_2}\right) e^{-jkr_2} \right|_{max} \quad for\ vertical\ polarization \right. \tag{5}$$

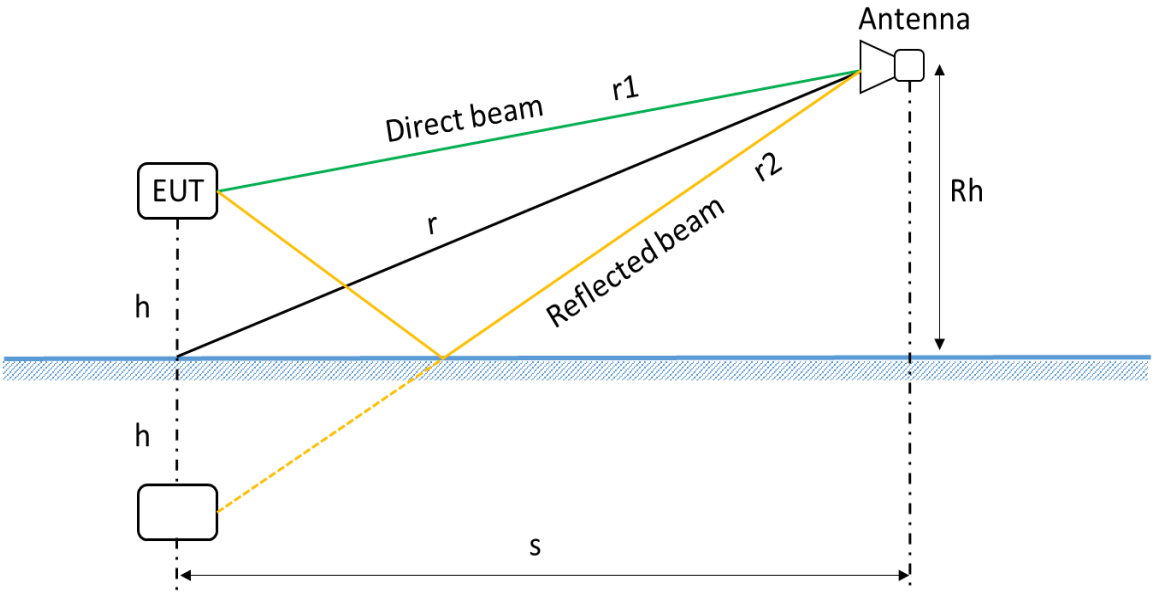

Figure 3.2. Geometrical factor g_{max} definition for radiated emission [6].

Where,

$r = \sqrt{s^2 + R_h^2}$	is the distance from the antenna to the perpendicular foot of the EUT (in m)

$r_1 = \sqrt{s^2 + (R_h - h)^2}$	is the length of the direct beam (in m)
$r_2 = \sqrt{s^2 + (R_h + h)^2}$	is the length of the reflected beam (in m)
s	is the measurement distance (in m)
R_h	is the antenna height (in m)

The maximum E-field strength is found by varying R_h over the range of 1-4 m with h of 1 m. For measurements at frequencies above 1 GHz, the standard requires placement of absorbers on the ground plane between the EUT and the receiving antenna. This eliminates the ground plane reflections and the r_2 terms in equations (4) and (5) . Average g_{max} over min. and max. R_h range for a fixed s is around 0.97. g_{max} can thus be approximated as 1 for simplification and this approximation is valid for any emission measurements above 1 GHz. Thus equation (3) now becomes:

$$E_{Max} = \left(\frac{\sqrt{30 \times P_{radiated} \times D_{max}}}{R}\right) \quad (6)$$

3.3 DIRECTIVITY

As the radiation pattern of an electrically large EUT becomes irregular at high frequencies, it becomes difficult to measure the maximum E field strength in a semi-anechoic chamber or OATS. The TRP measurement in reverberation chamber could simplify the measurement procedure and reduce the measurement time. However, to convert this measured TRP into equivalent E field strength of a standard emission measurements, directivity of the EUT has to be known.

Directive gain of any radiator is a measure of the radiated EM power as a function of aspect angle, referenced to the average isotropic value. The directivity of EUT can be a significant contributor to overall EMC measurement uncertainties, especially as the testing frequencies climb over the GHz range. This factor is a critical link between the TRP measurement in a RVC and equivalent E field conversion. Most of the test sites are validated using a Hertzian dipole and hence the D_{max} is assumed to be 1.55. As mentioned that the radiation pattern of an electrically large EUT becomes irregular at higher frequencies, therefore the assumption of dipole like radiation is typically insufficient and leads to an inaccurate maximum directivity. Also, electronic devices act as an unintentional radiators which means that it is not possible to know the direction of maximum radiation without performing a 3-D scan, however the directivity of the EUT has to be known in order to convert the measured radiated power into comparable maximum field strength of a standard emission measurement. In order to determine the directivity, radiation pattern measurement is necessary though it is very time consuming.

In many papers, stochastic approaches have been derived to describe the probability distribution of the directivity of an unintentional radiators. The directivity was defined to be chi squared distributed with two degrees of freedom commonly known as exponential distribution. The theoretical basis for the directivity of an unintentional radiator is spherical wave theory which is a function of the EUT electrical size (*ka*), where '*k*' is the wave number and '*a*' is the radius of the small sphere enclosing the entire EUT. Three approaches have been developed to estimate the directivity of an unintentional radiator:

3.3.1. Dmax Based on Spherical Wave Theory [1, 7]. The upper bound of an unintentional radiator is estimated as :

$$Dmax = \begin{cases} 3 & for\ ka\ \leq 1 \\ (ka)^2 + 2ka & for\ ka > 1 \end{cases} \quad (7)$$

Under the condition of $ka > 1$, the EUT is considered to be electrically large and this approach overestimates the actual directivity of the EUT. Thus this provides the upper bound of the D_{max}. For example, Figure 3.3 shows the directivity variation with frequency for an object of 1m maximum physical dimension.

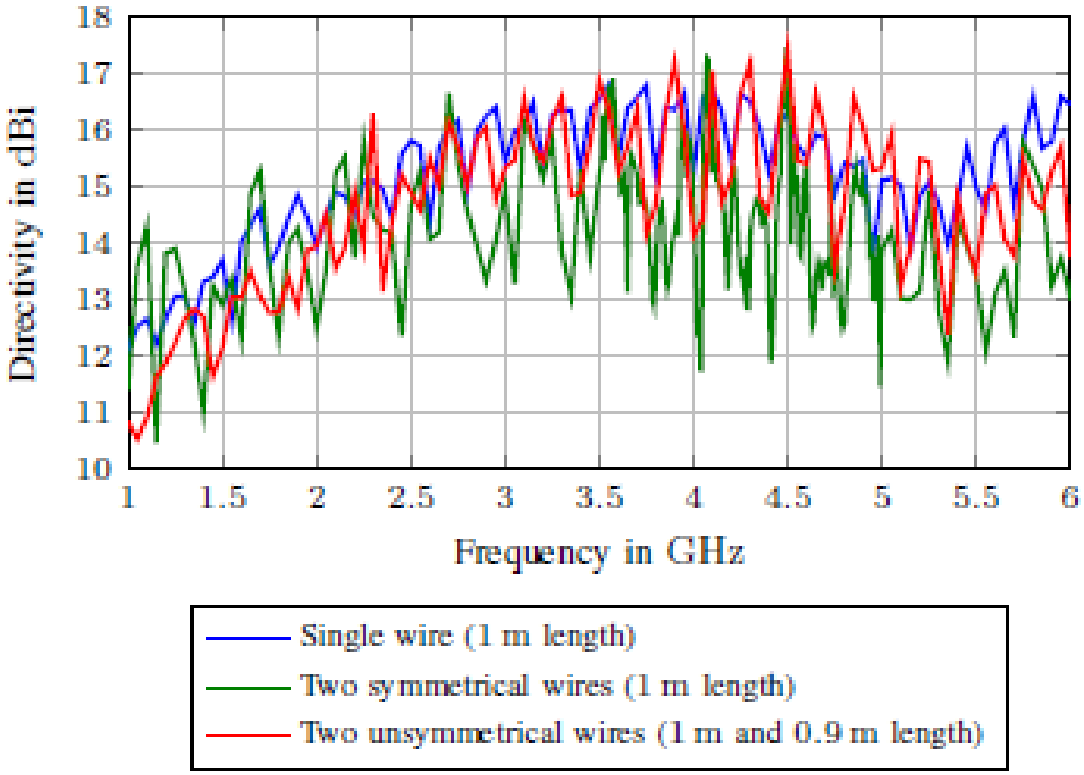

Figure 3.3. Simulated directivity against the frequency for an object [4]

If the directivity is simulated for an emitter element of maximum physical dimension 1m. Based on this real directivity from simulation, if 'a' is calculated using equation (7), the value of 'a' is too small than what it should be.

In this case, from the directivity we see that the value of 'a' is around 0.15m @1GHz and 0.025m @6GHz. However, the required 'a' should be 0.5m. Hence, the D_{max} will be higher than the real value because D_{max} is directly proportional to 'a' in the equation (7). Figure 3.4 shows the plot for variation of *'a'* calculated from equation (7) over the frequency range of interest.

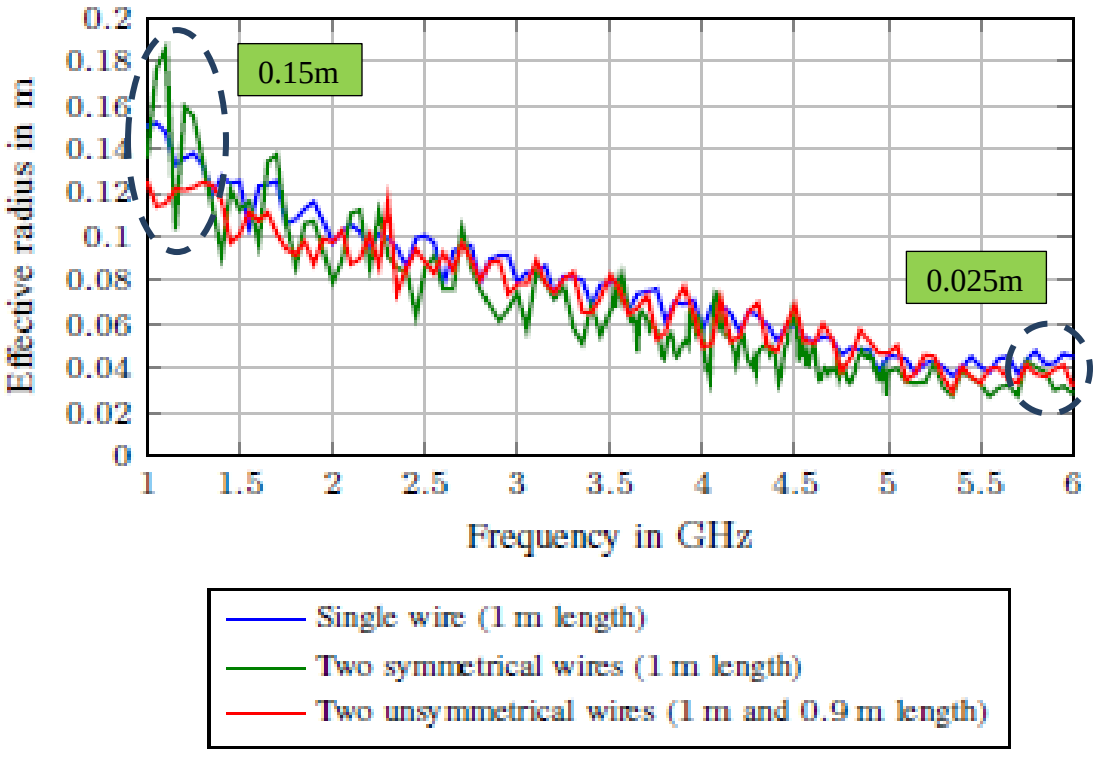

Figure 3.4. Effective radius against the frequency as per equation (7) [4]

Hence, if we were to plug in the real value of '*a*', which is 0.5m, the equation (7) will give us a directivity which is higher than the real value. The directivity is 130.6 for '*a*' = 0.5m @1GHz. Figure 3.5 illustrates the overestimated directivity with real value of '*a*' plugged into equation (7).

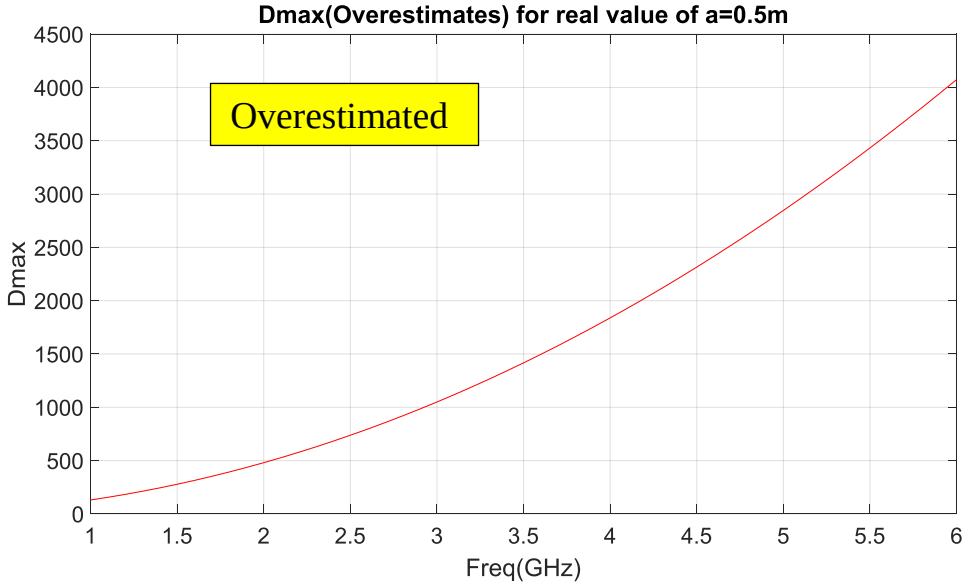

Figure 3.5. Overestimation of directivity based on the real value of *'a'* when applied to equation (7).

3.3.2. Statistical Expectation of the Maximum Directivity Based on Spherical Wave Theory [12]. The expectancy value of the maximum directivity statistically evaluated to be following the below expression:

$$Dmax = \begin{cases} 1.55 & for\ ka \leq 1 \\ \frac{1}{2}\left[\ln(4(ka)^2 + 8ka) + \frac{1}{8(ka)^2+16ka} + 0.577\right] & for\ ka < 1 \end{cases} \quad (8)$$

This expectancy value underestimates the actual maximum directivity and effective radius based on it would be too large to be physically viable. Similarly if the real value of 'a' is plugged in equation (8), the D_{max} value we get will be less than what it should be because D_{max} is inversely proportional to 'a'. The directivity is 3.42 for 'a' = 0.5m @1GHz. This is analyzed and shown in Krauthauser's thesis work: "Grundlagen und Anwendungen von Modenverwirbelungskammern". Figure 3.6 illustrates the understimated directivity with real value of 'a' plugged into equation (8).

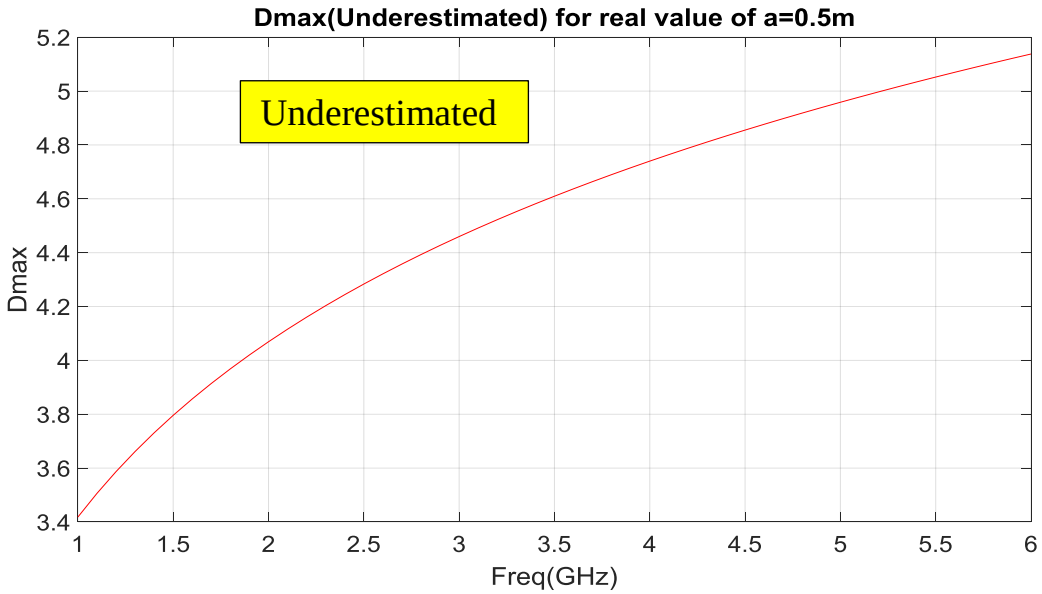

Figure 3.6. Underestimation of directivity based on the real value of *'a'* when applied to equation (7)

3.3.3 Maximum Directivity Based on TWA and SWA Theory [4].

The directivity in this approach is estimated using:

$$Dmax \approx 2.\frac{9.1\frac{a}{\lambda_0}-1.7}{2.1+ln\frac{a}{\lambda_0}} \quad (9)$$

This study was done to investigate the directivity and effective radius of an electrically large EUT with attached wires. This theory claims to deliver more reasonable values of 'a'. The directivity is 10.47 for 'a' =0.5m @1GHz. Figure 3.7 shows the variation of effective radius as per equation (9) based on TWA and SWA theory and Figure 3.8 shows the simulated value of D_{max}.

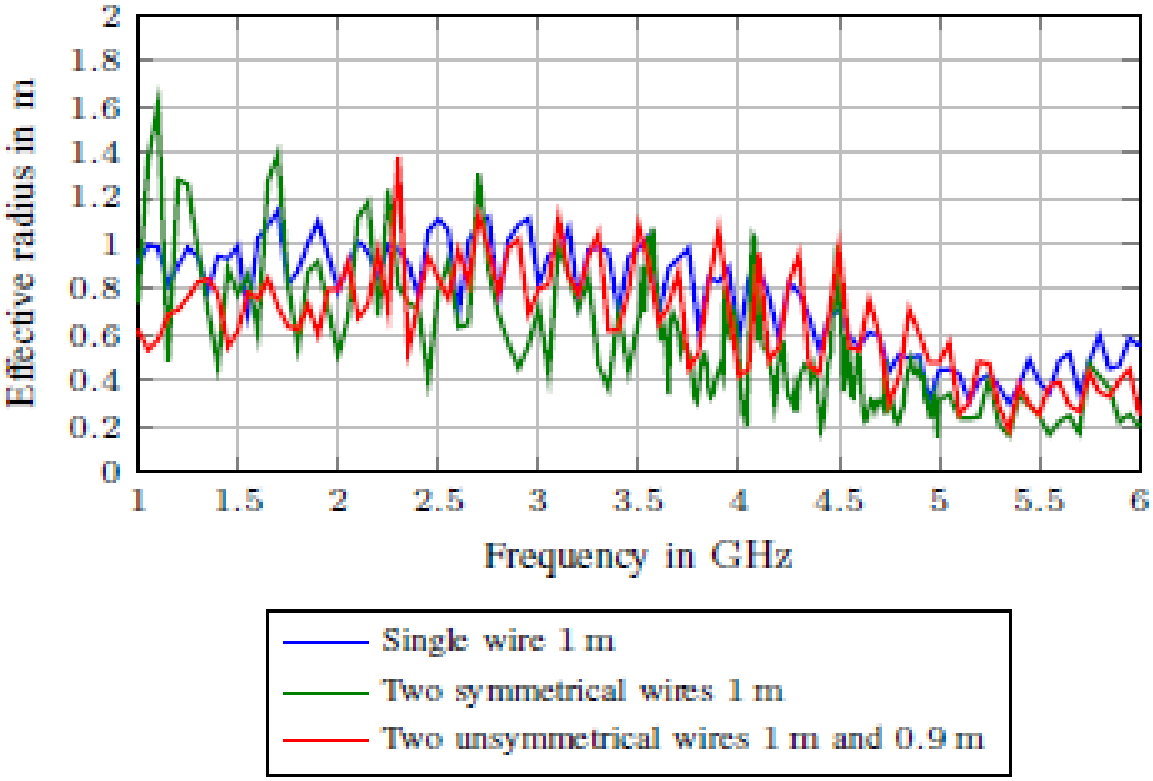

Figure 3.7. Effective radius against frequency as per TWA and SWA theory [4]

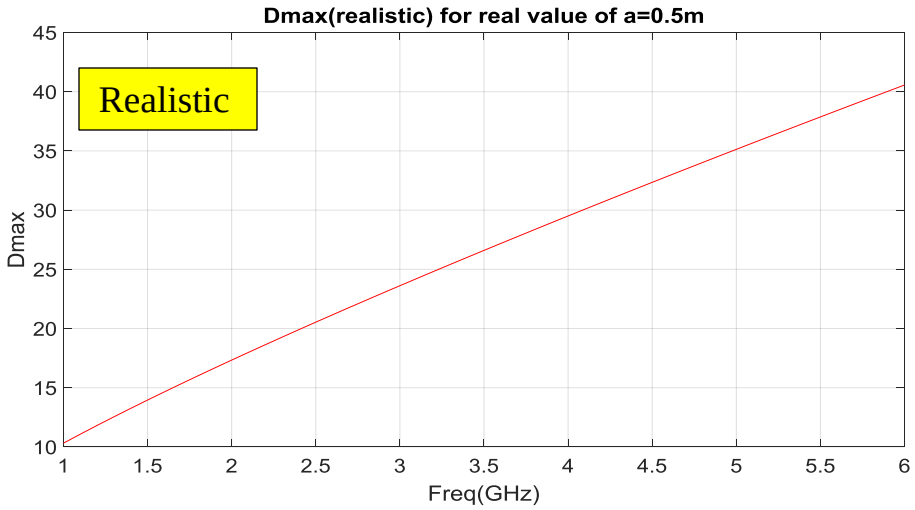

Figure 3.8. Simulated curve of D_{max} based on equation (9)

For this thesis's study subject, the maximum dimension is 0.54m, hence effective radius 'a' = 0.27m. The analysis is aimed at 10.3 GHz, therefore, ka = 56.5 >> 1, hence its electrically large. Using equations (7), (8) and (9) for the condition of ka>1 to calculate D_{max} with the real value of 'a' = 0.27m, we get the values as follows:

Equation (7) => D_{max} = 331.08

Equation (8) => D_{max} = 5.034

Equation (9) => D_{max} = 37.3

The total process of TRP to E field conversion can be summed up as follows: Radiation pattern measurement → Directivity estimation → E field conversion from the measured TRP using the relation between E_{Max} and $P_{radiated}$ mentioned above. Main contributing parameters for this conversion are g_{max} and D_{max}. g_{max} is a parameter of the test site which can be approximated to be equal to 1.

The general definition of max directivity is the ratio of maximum power density into a direction to the mean value of the radiated power density in all directions. This is given by the equation below as per [2]:

$$Dmax = max\left\{\frac{S_{co}(\theta,\varphi)}{\langle S(\theta,\varphi)\rangle}\right\} \quad (10)$$

The D_{max} estimation process needs to be validated through measurement to implement any of the above mentioned approaches. We can get $S_{co}(\theta,\varphi)$ from radiation pattern measurement because this term represent the power density in a particular direction as a function of the aspect angle (θ being the elevation plane and φ being the azimuthal plane), $\langle S(\theta,\varphi)\rangle$ represents the average power in all direction and can be derived from our TRP measurement in RVC using equation (2). The closest match between our measurement results using equation (10) and the theoretical results from the (7), (8) and (9) can be used for the purpose of D_{max} estimation in this study.

4. EMISSION GROWTH ANALYSIS APPROACH

The method of TRP conversion to equivalent E-field will be implemented to predict the growth of emission from multi-modular systems. However, the factors and parameters which influences the emission level from large systems needs to be analyzed and understood. For the purpose of analyzing EMI radiation from large systems, the approach can be divided into two levels: system level and modular level. For this study, two aspects were considered. The first is to determine the electromagnetic parameters of the sources which influences the emissions (modular level analysis) and the secondly to determine which electromagnetic principle should be used to describe the addition of radiation sources (system level analysis).

To investigate the accumulation effect, one needs to understand the radiation properties of the main radiating elements only and exclude the radiation from the sources that do not multiply like slots due to poor gaskets, mechanical defects in the chassis, irregular grounding contacts, etc. A networking equipment is used as our equipment under test (EUT). We leveraged the information of main radiating elements and their coupling paths in networking equipment concluded by [9] in our study. The frequency of interest for this study is 10.3 GHz.

5. TEST SUBJECT DESCRIPTION

During the entire course of this study, two high speed networking switches were used as the equipment under test (EUT). The modular level approach was carried out in a network switch which holds four optical transceiver modules (SFP+). This prevents the complication of multiple radiator present in a system when the focus of analysis is only on the major radiator elements (SFP+). These are plugged into the switch to enable data traffic, these SFP+ runs data at a rate of 10 Gbps. Figure 5.1 and Figure 5.2 shows the photos of EUT 1. Figure 5.3 shows a picture of optical transceiver module used in high speed routing and switching systems.

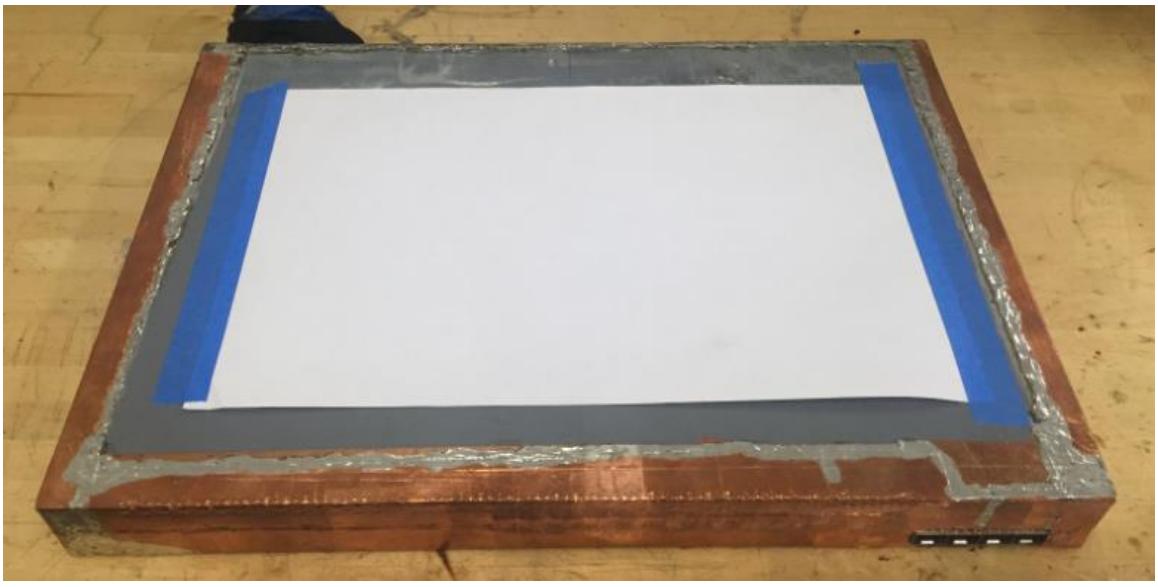

Figure 5.1. EUT 1 top view

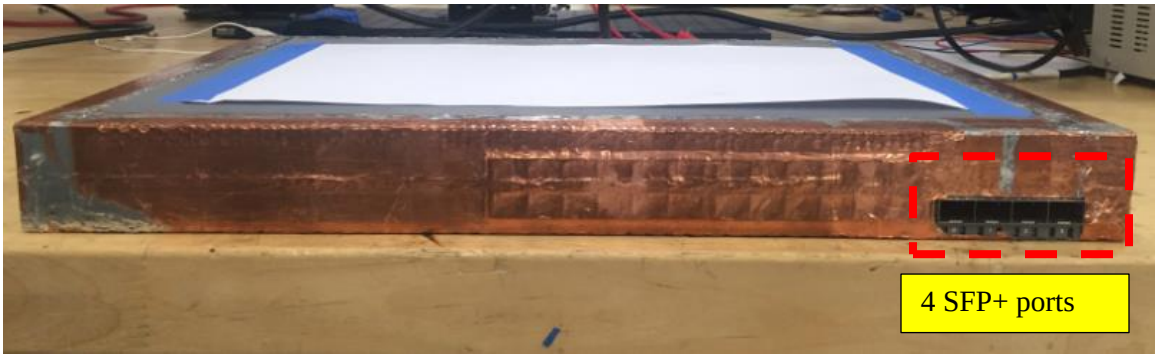

Figure 5.2. EUT 1 front view showing the ports for the four optical modules

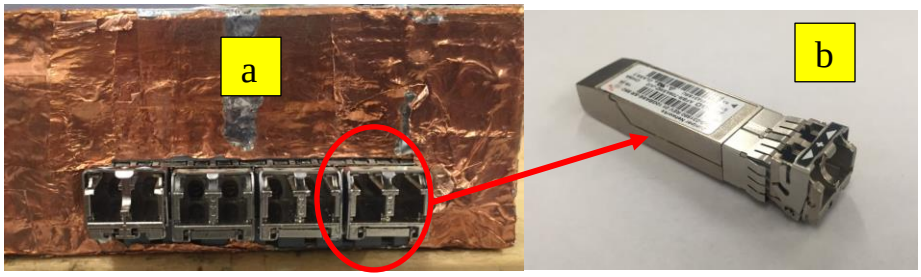

Figure 5.3. SFP+ port and module. (a) 4 optical modules plugged into the EUT 1 ports; (b) Optical transceiver module (SFP+) used in a typical networking systems.

EUT 1 was covered with copper tape to ensure the emission observed is only from the SFP+ modules and not from any slots, air vents or any other chassis mechanical anomalies. These SFP+ modules are manufactured by different vendors, so they have different mechanical designs, internal functionalities (laser power, optical to electrical transition, signal conditioning, etc.), shielding and grounding implementations. Though the main function of these transceiver modules is to facilitate the flow of traffic, but their implementation and design difference influences the radiated field. Studies have been conducted to investigate the radiation physics from these modules, thus this study have been carried on leveraging this information of the optical transceiver modules being the main radiating element in the high speed networking switches and routers.

For the system level EMI analysis, a larger switching system (EUT 2) was used to validate the accumulating effect when multiple of these optical transceiver modules are added. This network switch holds up to 16 line cards and each line cards has 36 transceiver ports. This large system uses an advanced optical transceiver module which is called the QSFP+. The data rate is higher than SFP+ modules and can go up to 100 Gbps, but for EUT 2, QSFP+ modules with 40 Gbps data rate was used. QSFP+ has 4 channels and each channel has a data rate of 10 Gbps, so it aligns with the frequency of interest for this study. Figure 5.4 shows the actual photo and physical layout of EUT 2, Figure 5.5 shows the one line card from EUT with optical modules plugged into it.

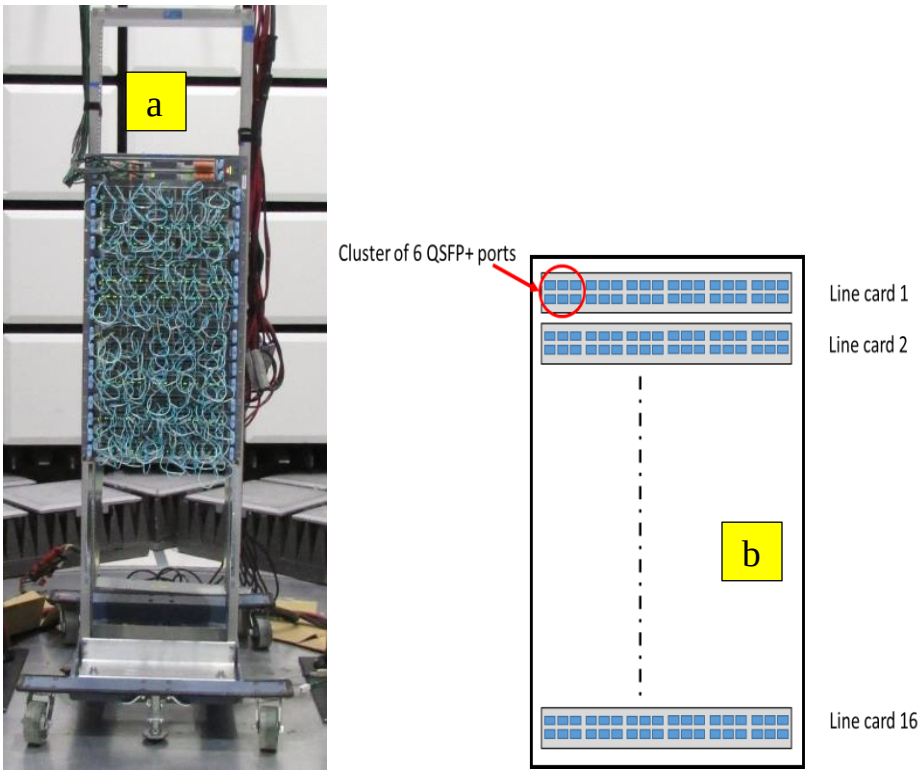

Figure 5.4. EUT 2 description. (a) EUT 2 front view with all the 16 line cards and QSFP+ modules populated; (b) Physical layout of the EUT 2 showing line cards and QSFP port clusters

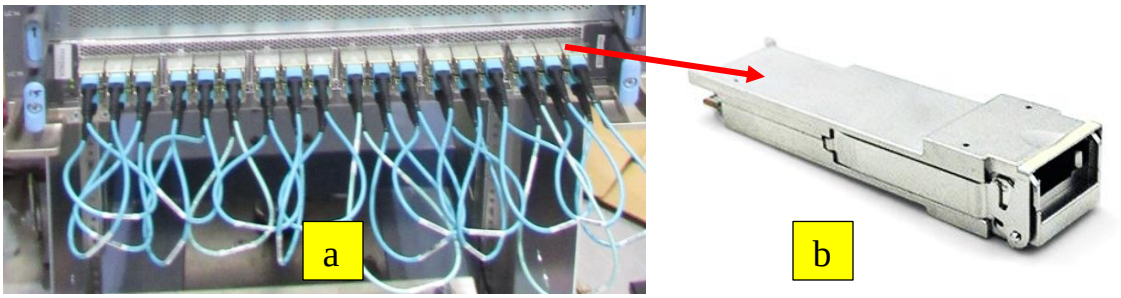

Figure 5.5. QSFP + ports and module. (a) One line card plugged in with 36 optical modules. (b) Optical transceiver (QSFP+) module used in EUT 2.

6. CHARECTERIZATION OF THE RADIATING SOURCE

In this study, there are two different possibilities: Firstly, if all the sources radiate at the same frequency, then the EM principle of array antenna theory can be applied for analyzing the growth of emissions from addition of multiple modules. In an antenna array, geometrical configuration of the elements, excitation amplitude, phase relationship between them and their individual pattern influence the overall pattern. This forms one large array antenna and voltages are added as a result of addition of subsequent radiating sources. Secondly, if the frequencies are slightly different, beat frequencies will be created, and then the superposition principle has to be applied where power is added and averaged instead of voltages. This includes the effect of receiver instrument settings of resolution bandwidth (RBW) and the detector type.

For this study, from the frequency scan it was observed that the main radiation is around 10.3 GHz. However, all the optical transceiver modules in one line card radiate at exactly the same frequency which forms one array antenna system. But all the optical transceiver modules in other line cards radiates slightly off from 10.3 GHz, within a few kHz apart. Thus, the system forms multiple array antenna system comprising of each line card as single array antenna system. For example, if such a network switching system has 4 line cards plugged into it, it forms 4 different array whereas a system hosting only 1 line card will form 1 array. This study concentrates on both the mentioned scenarios.

As per the approach adopted for this study to convert TRP into comparable E-field, some of the parameters in equation (6) needs to be investigated and learnt through measurements. According to antenna theory, an array system is characterized by the phase relationship between each elements, amplitude of excitation and geometrical

configuration. Also, to validate the D_{max} approach as per equations (7), (8) and (9), determining the radiation pattern of the main radiating element is necessary.

6.1 PHASE RELATIONSHIP BETWEEN RADIATING ELEMENTS

If in a multi-modular system each clock is created by its own PLL, then with every power cycle the PLL may lock at a different phase value and produce random phase variations between the modules. Phase relationship influences the main beam of the radiation based on the constructive and destructive interference. To see the accumulation effect, pattern multiplication concept is applied [10], where the total E field of an array is a vector superposition of the fields radiated by the individual elements multiplied by the array factor.

The E_{Max} observed during a radiated emission measurement is a function of the main beam in the overall radiation pattern. When all elements are in phase, E_{Max}will increase significantly due to constructive interference, but if they are out of phase the resultant E_{Max} will decrease. From a system level point of view, determining the phase relationship between the elements in a multi-modular system is important.

In case of random phase distribution, if we assume the amplitude of excitation is same, the TRP may increase by 3dB for doubling of elements due to addition of power as shown in Figure 6.1, but not for E_{Max} as shown in Figure 6.2. There could a variation of as large as 12 dB in E_{Max} extrapolation between in phase and random phase distribution. In the EUT under investigation, the architecture doesn't define any control over the phase of the optical modules. Also, phase measurement of the modules relative to each other

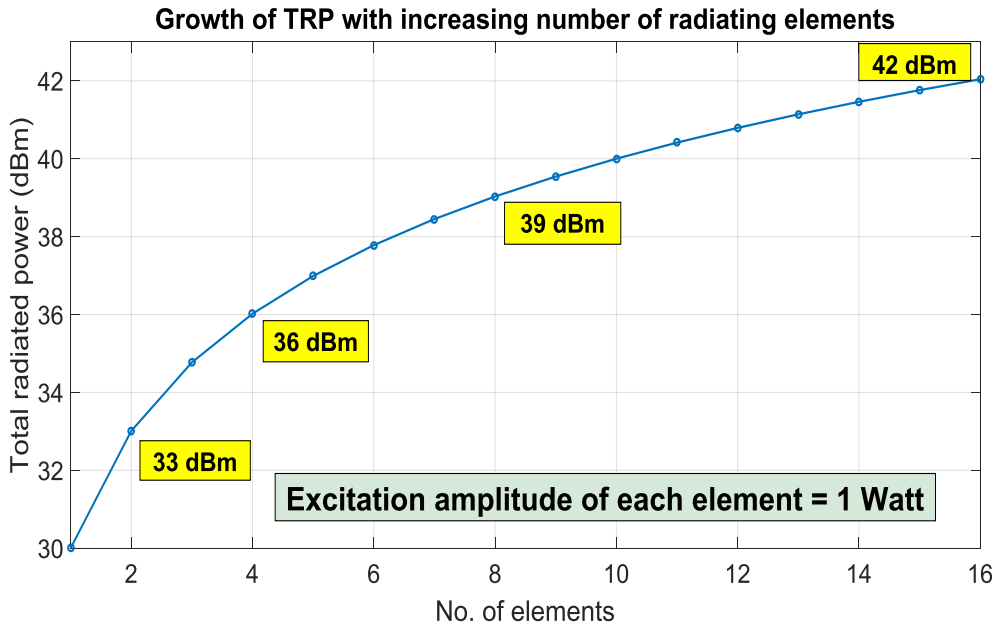

Figure 6.1. Simulation result showing TRP increases by 3dB for every doubling of elements. The elements were excited with same amplitude of power.

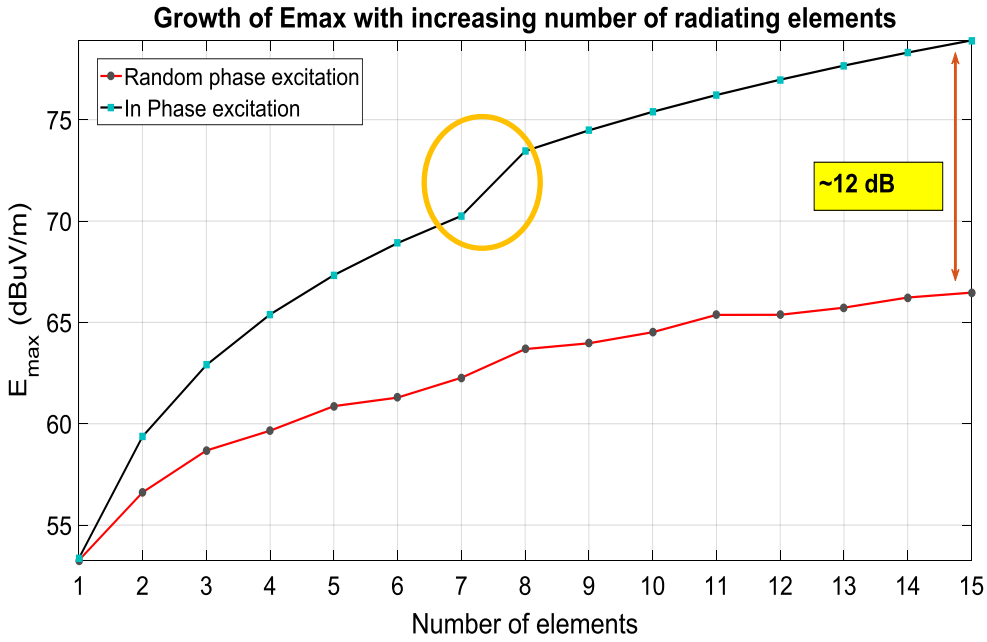

Figure 6.2. Simulation results showing growth of E_{Max} for in phase and random phase excitation for increasing number of elements. The simulation uses the TRP data, maximum directivity (D_{max}) of one optical module and extrapolates for 15 line cards plugged in a networking equipment. First 7 line cards hosts 30 optical modules each, whereas from 8th to 15th line card, each hosts 36 optical modules. The mutation from 7th to 8th line card as circled is due to sudden increment in the number of radiating elements.

was found to be random but fixed with every power cycle. Such randomness will be used in the statistical analysis input parameter.

6.2 RADIATION PATTERN FOR D_{max}

To predict the radiated emission in the height scan of 1-4 m, the knowledge of radiation patterns in both polarizations of these elements is needed. If the main beam falls in the scanning area of the receiving antenna, the measurement will capture the E_{Max} . If the main beam is at an angle beyond the scanning height, it is easy to miss the E_{Max} . Depending on the phase relationship between the modules, the resultant beam formation will be different when multiple modules are plugged in than beam formation from a single module. Because phase relationship was found to be random between them, the pattern information from one module can be used as an input for statistical simulation with randomization of the phase parameter.

Radiation pattern measurement was performed in an OTA chamber to obtain the 3D pattern of each radiating element. To validate the radiation pattern measurement setup, a radiating structure of X-band horn antenna is used whose radiation pattern is known. Figure 6.3 shows the setup diagram for radiation pattern measurement inside an Over the Air chamber (Anechoic chamber).

Figure 6.4 and Figure 6.5 shows the radiation pattern measurement setup arrangement details. Initial Position of the Horn antenna @ theta =0 and phi = 0;
X band horn antenna and the receiving horn antenna both are in horizontal polarization.

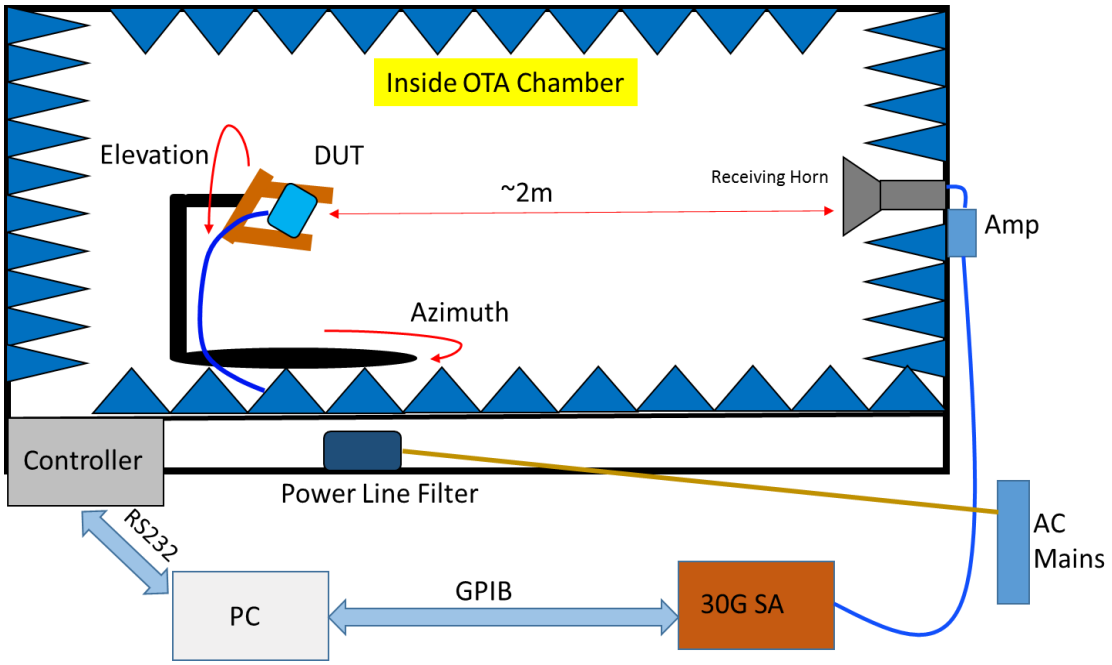

Figure 6.3. Setup details for the radiation pattern measurement inside the OTA chamber.

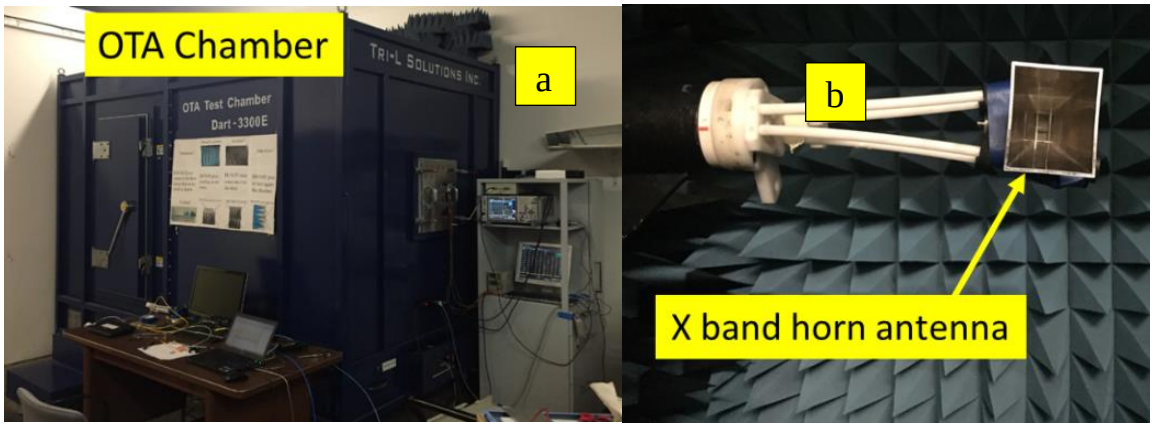

Figure 6.4. Radiation pattern measurement setup (a) The OTA chamber used for the radiation pattern measurement. (b) Photo showing the initial position of the X-band antenna.

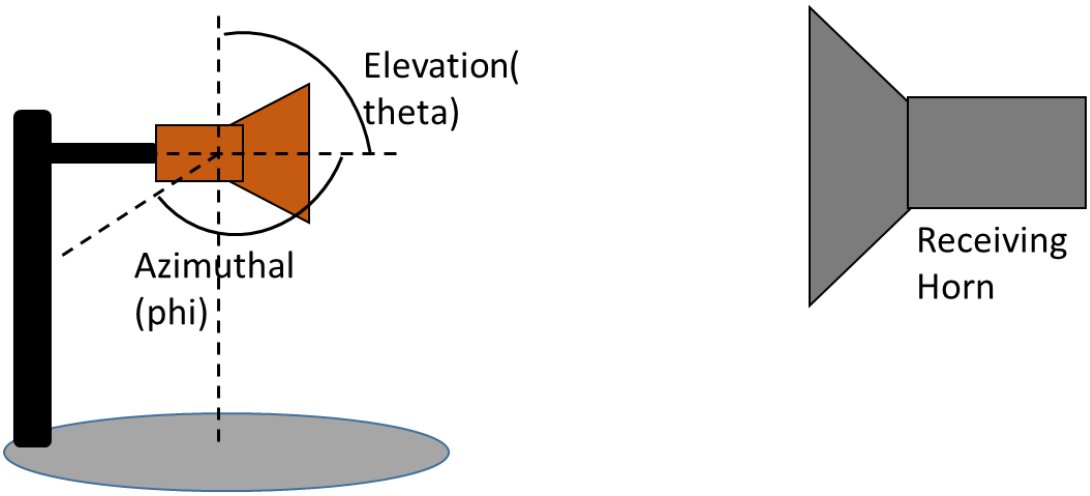

Figure 6.5. Arrangement of the horn antenna inside the OTA chamber for radiation pattern measurement.

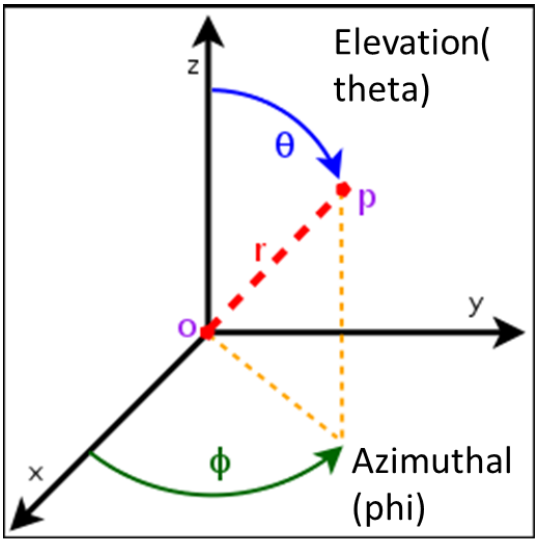

Figure 6.6. Coordinate system describing the plane of rotation for the radiation pattern measurement setup inside the OTA chamber.

Figure 6.6 shows the coordinate system used for our radiation pattern measurement. Expected max will be at:

1. Phi = 270, theta =0
2. Phi = 90, theta = 180

Because as per the EUT rotational fixture, the x band horn antenna will face the receiving antenna at 270 degree (phi) and the back of the x band horn antenna will face the receiving antenna at 90 degree (phi). The X band horn antenna was rotated in both azimuthal as well as elevation plane.

Elevation plane rotation = 0:10:360 degrees

Azimuthal plane rotation = 0:10:360 degrees

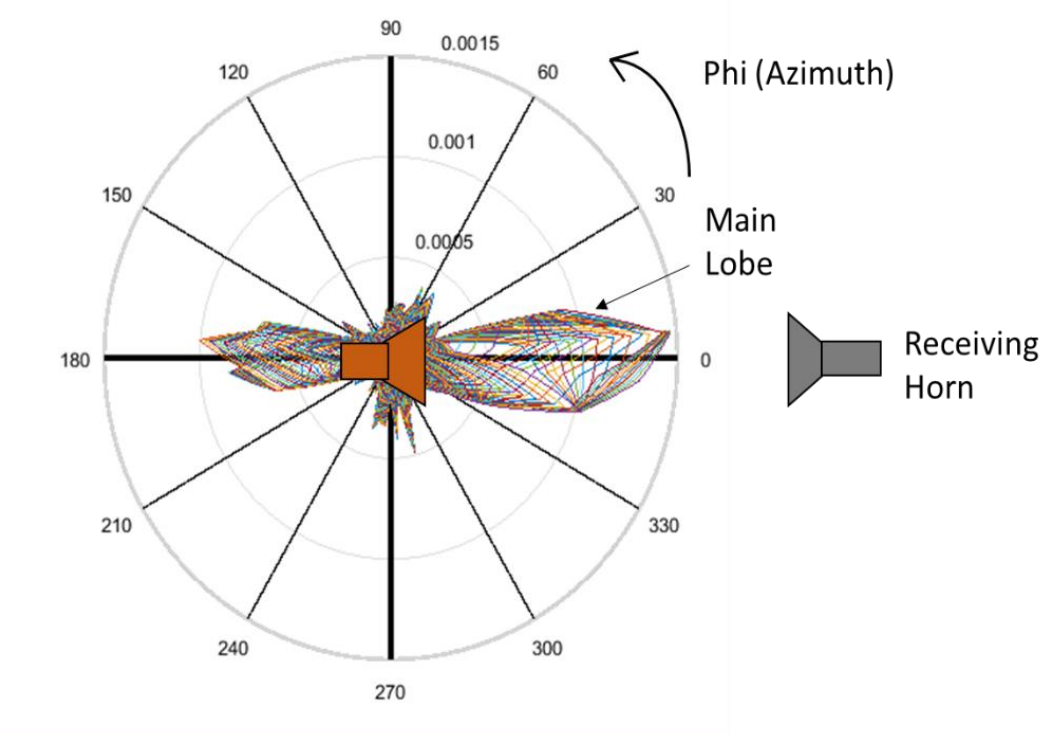

Figure 6.7. Polar plot for the X band horn antenna radiation pattern obtained from the measurement.

The above polar plot in Figure 6.7 shows the variation of phi (azimuthal plane) from 0 → 360 for every theta steps (elevation plane). The power is converted to linear values and 90 degree offset has been added to the axis in the plot to adjust the positioning of the rotational fixture for the EUT.

The linear plot in Figure 6.8 also shows the max occurring at phi = 90 and 270 degrees as per the expectation. Each curve of different color represents different steps in the elevation plane. Thus, this test result matches the expectation and verifies our test setup and the systems involved.

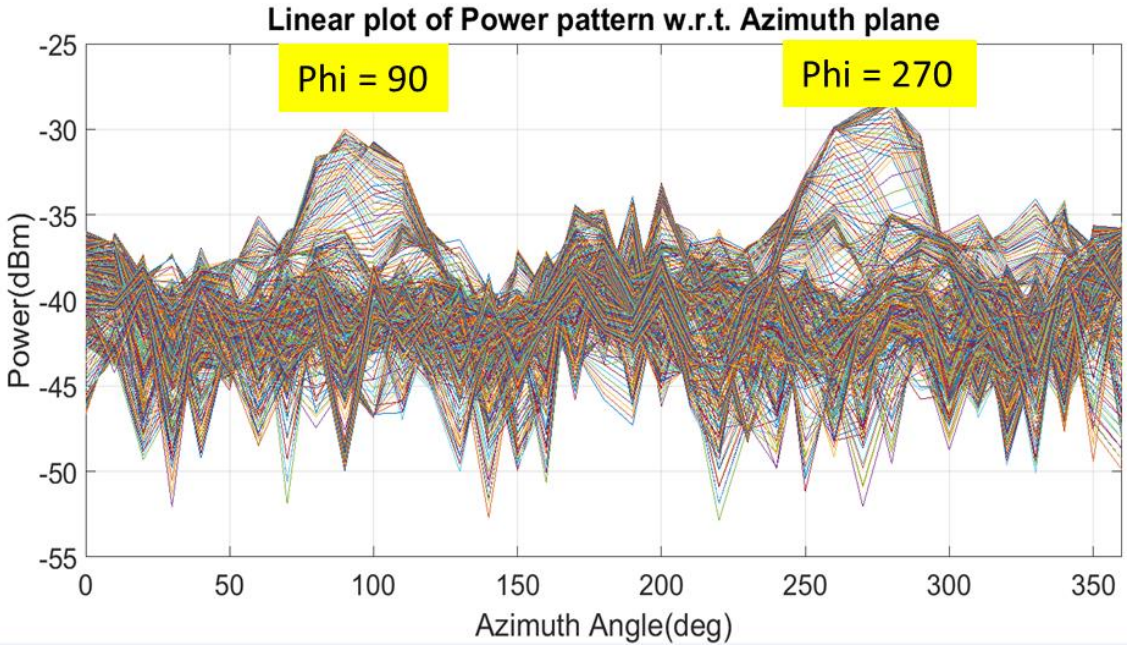

Figure 6.8. Linear plot of the radiation pattern of the X band horn antenna

The verified setup was used to fix the EUT 1 with just one optical module plugged in to measure its 3D radiation pattern as shown in Figure 6.9.

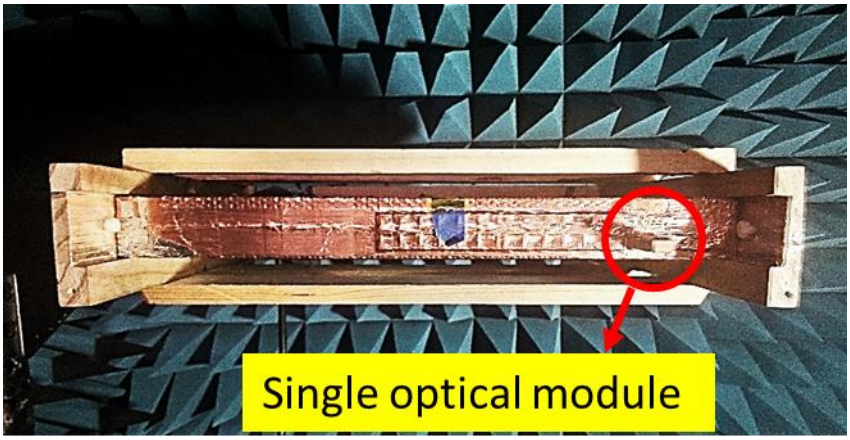

Figure 6.9. Fixture holding the EUT 1 inside the OTA chamber rotating arm for the optical module radiation pattern measurement.

Similarly, the initial position for the EUT 1 fixture is the same as that of the X band horn antenna. The front of the EUT 1 faces the receiving horn antenna when the rotational fixture is at 270 degree in phi direction (azimuthal plane). Optical transceiver modules from two different manufacturers were tested for their radiation pattern in both polarization (Horizontal and Vertical) of receiving antenna. Figure 6.10 shows the 3-D radiation pattern of the two different optical modules.

The radiation pattern of modules from two different manufacturers were measured and are compared in Figure 6.10 for both horizontal and vertical polarizations. The pattern plot in Figure 6.10 shows that the modules from different manufacturer have similar, but different radiation patterns. In vertical polarization both have one strong main lobe, but the pattern has multiple side lobes of comparable strength in the horizontal polarization. The main lobe in the vertical polarization for both the modules are facing the receiving antenna, which shows that the radiation from the modules are mainly frontal.

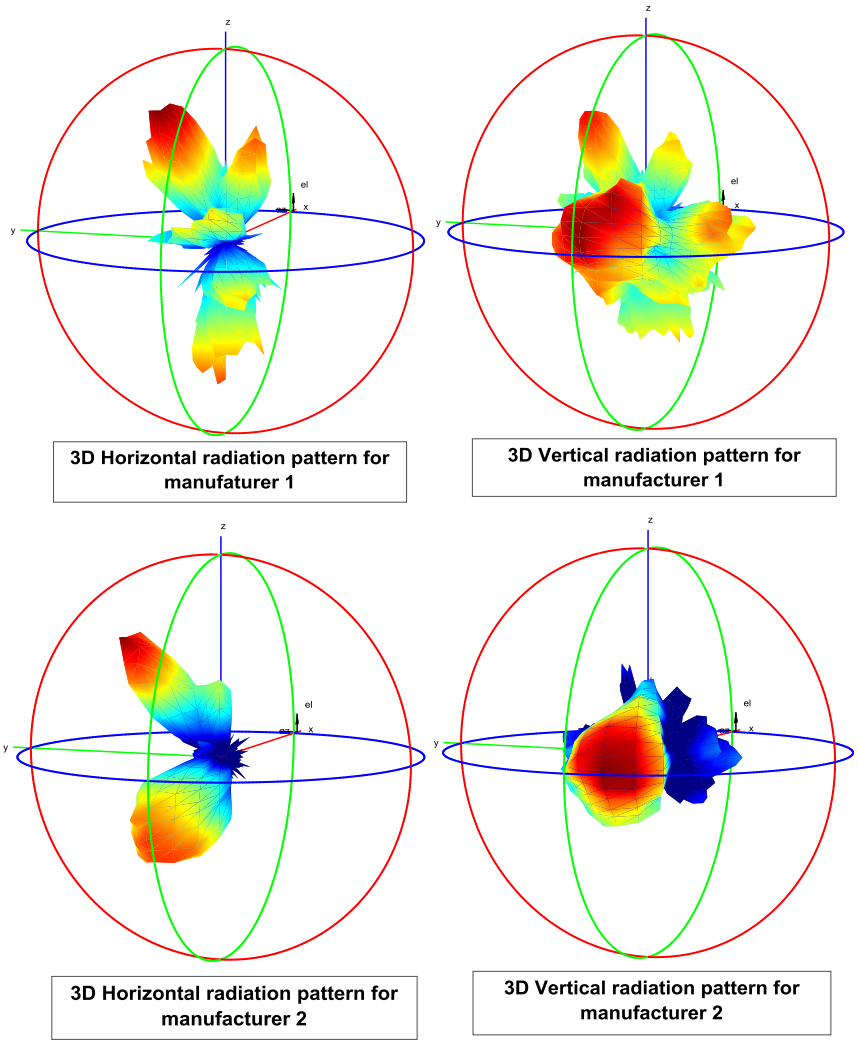

Figure 6.10. 3D radiation pattern of one optical transceiver module from 2 manufacturers showing similar horizontal and vertical radiation pattern.

In the horizontal polarization there are multiple side lobes mostly at angles which are not covered by the scanning antenna. The maximum angle that can be covered by the antenna is 52 degrees for 3 m distance, and as the distance of the antenna from the DUT increases, the angle of coverage decreases.

Hence, the radiation pattern for only the vertical polarization is considered in this study as the E_{Max} is likely to appear within the scanning range.

D_{max} theoretically defined by equation (10) can be simplified as below for calculation purpose from radiation pattern measurement of the modules:

$$Dmax = \left\{\frac{P_{max}(\theta,\varphi)}{P_{avg}(\theta,\varphi)}\right\} \tag{11}$$

Where,

$$P_{max}(\theta,\varphi) = \max\left(P_h(\theta_n,\varphi_m) + P_v(\theta_n,\varphi_m)\right) = -100.5488\ dBm \tag{12}$$

$$P_{avg}(\theta,\varphi) = \frac{\pi}{2NM}\sum_{n=1}^{N}\sum_{m=1}^{M}\left(P_h(\theta_n,\varphi_m) + P_v(\theta_n,\varphi_m)\right)\sin\theta_n = -111.7021\ dBm \tag{13}$$

Therefore from radiation pattern measurement, $D_{max} = 11.15\ dB$.

Based on the main radiating element size, the maximum radius ‘a’ to enclose the element is 0.05 meters. Comparing the three mentioned theoretical approaches for D_{max} estimation for ‘a’ = 0.05 meters, the 3rd approach based on TWA and SWA theory [4] yields the closest value of $D_{max} = 10.32\ dB$ at 10 GHz.

However after radiation pattern measurement of multiple different modules, D_{max} was found to be in the range of 8.76 dB to 11.15 dB.

7. ESTABLISHING RELATIONSHIP BETWEEN TRP AND E_{Max}

The measured pattern information is used to get the maximum directivity (D_{max}) of the radiating source, then E_{Max} is calculated from the measured TRP as per (1) and (2) respectively; where D_{max} is the maximum directivity of the radiating element obtained from equation (11), $P_{max}(\theta, \varphi)$ is the maximum power received as a function of azimuth (φ) and elevation planes (θ). $P_{avg}(\theta, \varphi)$ is the average power over the entire scanned area as a function of azimuth (φ) and elevation planes (θ).

$$E_{Max} = \left(\frac{\sqrt{30 \times P_{radiated} \times D_{max}}}{R}\right) \tag{12}$$

where, E_{Max} is the maximal E field strength, $P_{radiated}$ is the measured total radiated power (TRP), D_{max} is the calculated maximum directivity, and R is the distance of receiving antenna at which E_{Max} is estimated.

TRP is measured, while directivity is calculated based on the radiation pattern measurement. If we measure TRP from one module and assume that doubling the number of the modules will cause the TRP to increase by 3 dB, based on the radiation pattern from multiple modules considering the phase randomness, a reasonable extrapolation of E_{Max} can be achieved. To validate this approach, the measured and calculated TRP from E_{Max} of one module is compared. Figure 7.1 and 7.2 shows the setup for TRP measurement using one module in EUT 1 and the actual photo of the measurement setup inside the reverberation chamber respectively.

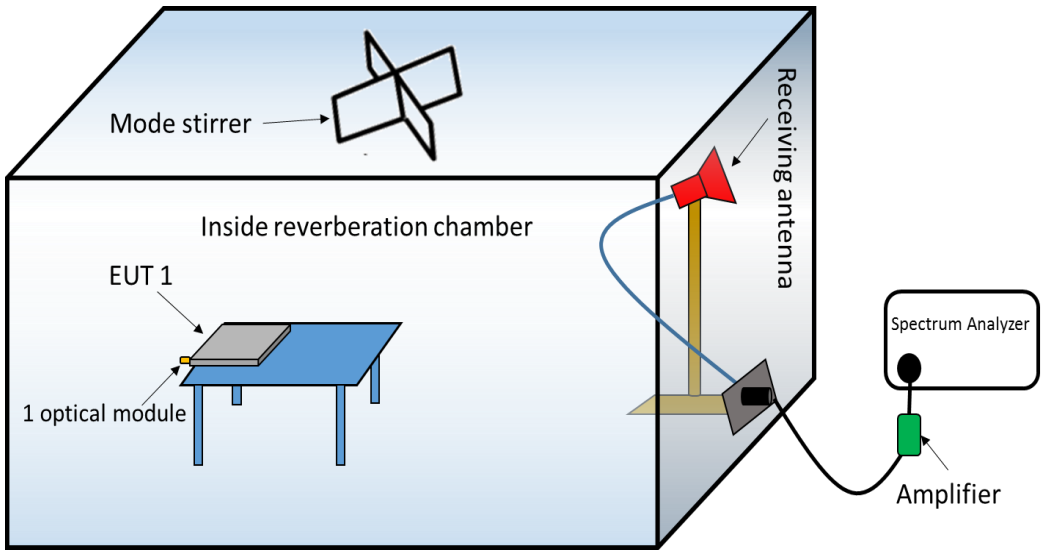

Figure 7.1. Setup diagram of the TRP measurement inside a reverberation chamber.

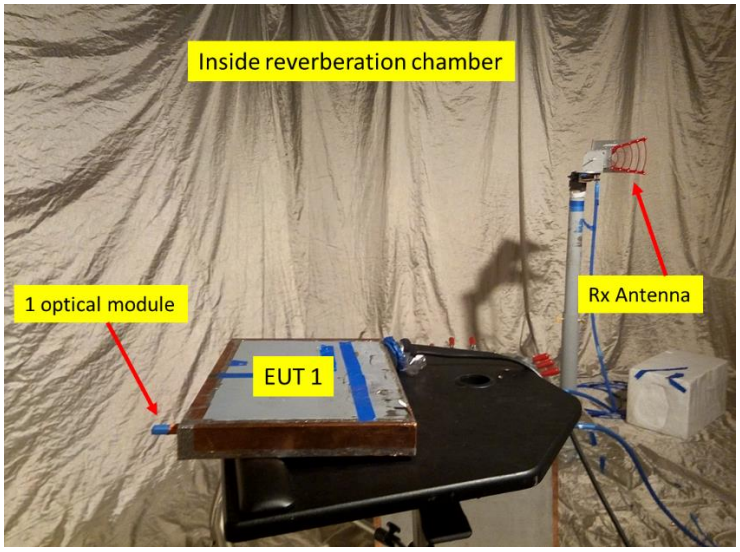

Figure 7.2. Actual photo of the measurement setup inside the reverberation chamber.

The reverberation chamber was characterized for chamber loss before placing the actual DUT. This loss will be compensated in the final TRP measurement reading. The EUT 1 was running traffic through one optical module plugged in and a horn antenna (750 MHz – 18 GHz) was used as the receiving antenna for the total radiated power. The

walls were shaken to homogenize the field inside the chamber. Table 7.1 shows the parameters and their obtained values from the TRP measurement and chamber characterization.

Table 7.1. Parameters from TRP measurement and chamber characterization

Parameters	**Description**	**Value**
$P_{received}$	Power received by spectrum analyzer	-88.511 dBm
Cable loss	System loss of all cables and adapters	10.686 dB
Amplification	Amplifier gain	39 dB
Chamber loss	Loss in RC chamber	47.3 dB

$$P_{Radiated} = P_{received} - \text{Amplification} + \text{Cable loss} + \text{Chamber loss} = -69.5\ dBm$$

Therefore, E_{Max} calculated from TRP measurement is *36.2 dBμV/m*.

To validate this E_{Max}, E field measurement at 3 meter distance has been carried out in a semi-anechoic chamber. Figure 7.3 and 7.4 shows the setup diagram and actual photo respectively for the E field measurement at a distance of 3 m inside a semi-anechoic chamber.

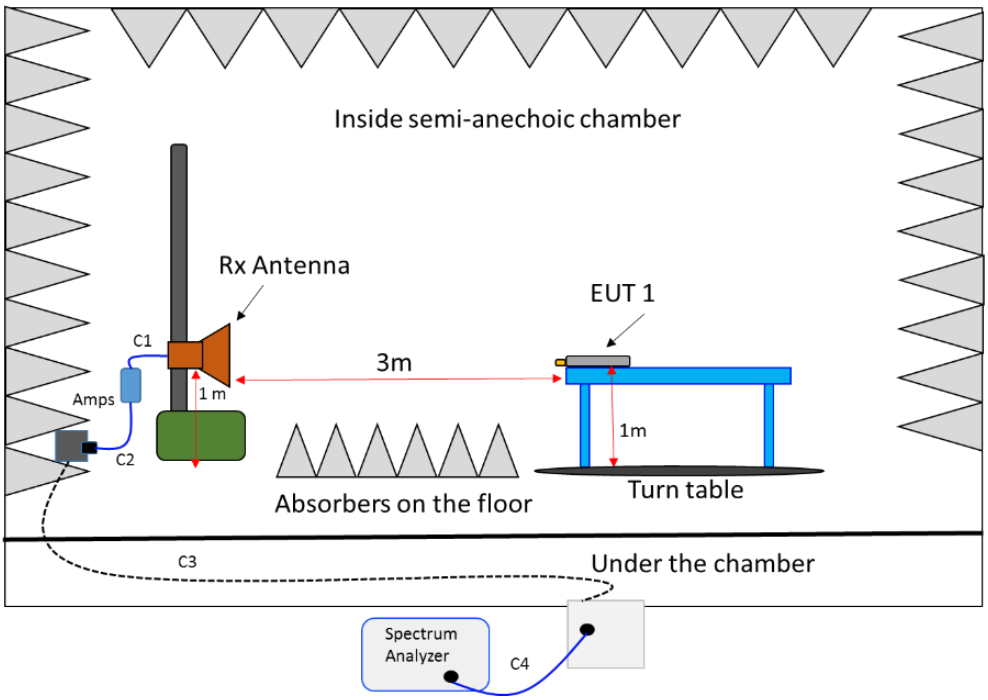

Figure 7.3. Setup diagram for E field measurement inside semi-anechoic chamber

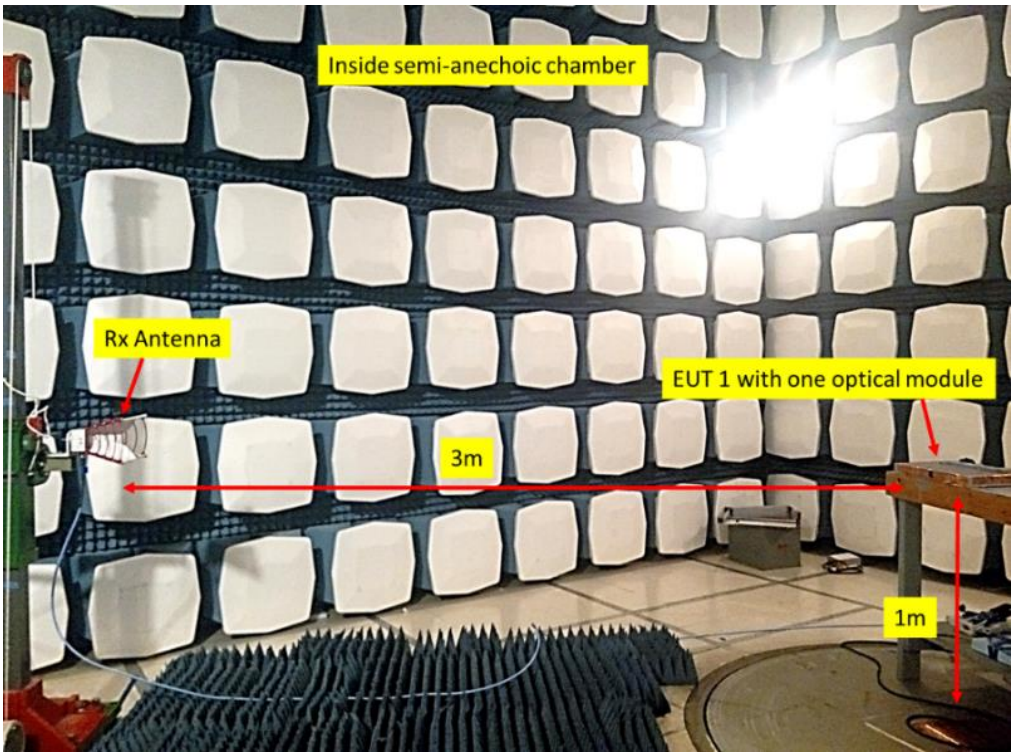

Figure 7.4. Actual photo of the setup inside the semi-anechoic chamber for E field measurement of one optical module in EUT 1.

Electric field measurements above 1 GHz in a semi-anechoic chamber requires placing of absorbers on the floor. The Rx antenna height was varied from 1- 4 meter and for every height in steps of 0.5 meter, the EUT 1 was rotated 360 degree using the turn table.

The E_{Max} recorded from the measurement was 37 dBµV/m after compensating the amplifier gain and cable losses. The value is in close agreement with our calculated E_{Max} from the TRP measurement within experimental and measurement uncertainties. Thus, the relationship between TRP and E_{Max} is established for one optical module from its 3D radiation pattern measurement and TRP measurement.

8. STATISTICAL SIMULATION FOR THE EMI GROWTH ESTIMATION

After the characterization of the main radiating elements, array antenna theory has to be implemented through simulation. The EM properties of the main radiating elements is used as the input parameter to this simulation. For evaluating several indices in a complex and large system such as the networking switches and routers which holds multiple high speed similar hardware, statistical approach has been adopted. As mentioned, this study deals with two scenarios: optical modules in one line card radiates at the exact same frequency but when multiple line cards are present in such complex system, each of them are at a slightly different frequency. Meaningful phase relationship can be established within a line card between the optical modules, but due to offset in the radiating frequencies among multiple line cards the phase will be a random variable. Also, the directivity of the modules were observed to vary in a range of 8.76 dB to 11.15 dB. The Monte Carlo simulation is one method to model the probability of different outcomes in a process that cannot be predicted easily due to intervention of random variables. Its evaluation allows for risk analysis by producing possible outcomes by implementing a range of values and uncertainties involved in a system. The objective is to obtain a reasonable extrapolation of E_{Max} taking into account the randomness of the parameters which influences growth of E field. This study implements phased array antenna theory as the model for the Monte Carlo simulation to estimate the maximum emission.

8.1 ARRAY ANTENNA THEORY IMPLEMENTATION

The test subject under investigation in this part of the study is EUT 2. This EUT holds similar multiple line cards, where each line card's radiating frequency is slightly different from each other. Without paying attention to the mutual coupling effects for an array of N combined identical antennas on a 3- dimensional space(x_n, y_n, z_n), one can express E field at a specified distance from the array antenna as below:

$$E(\theta, \varphi) = \sum_{n=1}^{N} E_{\max\_n} E_n(\theta, \varphi) e^{jk\psi_n} \quad (13)$$

Where,

$E_{\max\_n}$	is the maximum E field strength for each element
$E_n(\theta, \varphi)$	is the radiation pattern for each radiating element
$\psi_n = x_n \sin(\varphi)\cos(\theta) + y_n \sin(\varphi)\sin(\varphi) + z_n \cos(\varphi)$	is the phase correction for adjacent radiating elements

Therefore, by considering the geometry of phased array antenna structure, the element radiation pattern and the element E_{Max} , one can calculate the total emission growth at a specified distance from a large system hosting multiple similar subsystems.

For the system under study (EUT 2) with random phase distribution between the radiating elements, Monte Carlo algorithm [13] is applied as per the below block diagram in Figure 8.1. Therefore, by means of each element characteristics, it is possible to

estimate an overall behavior of a fully loaded system using few sampled E_{Max} according to EMC standard.

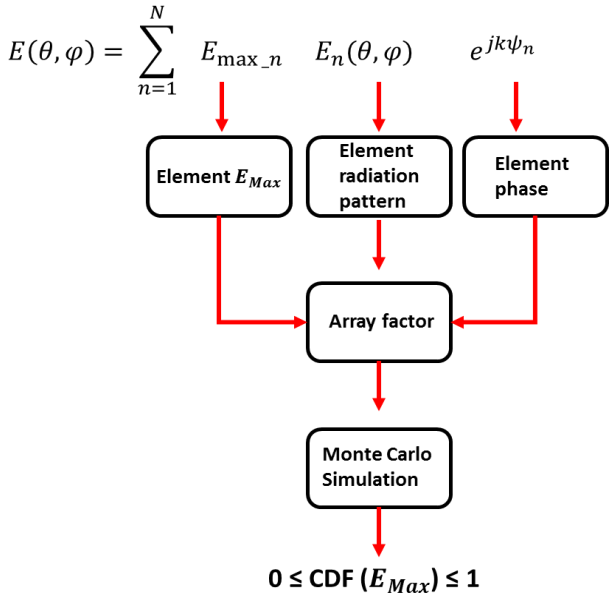

Figure 8.1. Statistical analysis block diagram using Monte Carlo simulation in order to predict the total emission for a large number of radiators.

In this block diagram, the radiating element's maximum radiated emission, radiation pattern and phase information are the input parameters to the simulation and the output of the simulation is a Cumulative Distribution Function (CDF). Cumulative Distribution Function was chosen as the output of the simulation due to the randomness of the input variables. The simulation aims at estimating the growth pattern from a large system when multiple similar hardware modules are added, so the end result is not a specific number but a probable range of E_{Max} values. Since, the phase relationship between the radiating elements is completely random, an exact value cannot be obtained

and hence neither a probability distribution. Hence, to implement such randomness in an estimation algorithm, CDF is best suited to fit the number of occurrences equal to or less than a specific value. CDF is the integral of PDF and both yields similar results but the CDF data representation is more easily comprehensible than PDF in this case.

According to the block diagram and using antenna array theory, one can apply the random distribution for all cases including radiation pattern, amplitude and phase. For this study, only concentration was the random phase distribution to find the CDF of E_{Max} based on the array geometry.

EUT 2 was hosting two types of line cards in it, type 1 had ports for 30 optical modules and type 2 had 36 ports. From top to bottom as shown in Figure 8.2, first 7 line cards were of type 1 and the rest 8 were of type 2. This is a fully loaded system with 498 optical transceiver modules radiating around 10.31 GHz.

The radiation pattern measurements as performed earlier showed that the vertical polarization has a clear main lobe with a beam width of around 30 degrees whereas the horizontal polarization had multiple lobes at an angle which is not covered by the antenna scan of 1-4 m. The peak amplitude in vertical polarization was also 4-5 dB higher than horizontal polarization when tested with multiple sample of modules from different manufacturers. This study is concerned with the worst case scenario which directs us to concentrate on the maximum E field emission. Therefore in vertical polarization, the radiators have the main lobe which will be captured by the scanning antenna and also higher amplitude, it is considered as the worst case (dominant case). The architecture of these systems doesn't define any control over phase of the signals which are fed into these optical modules and it was also confirmed by near field phase measurements. Thus,

it is rational to use the input parameter of phase as a random variable into the MCS simulation. Figure 8.2 shows the geometrical details of EUT 2 to be applied into the array antenna system for the simulation.

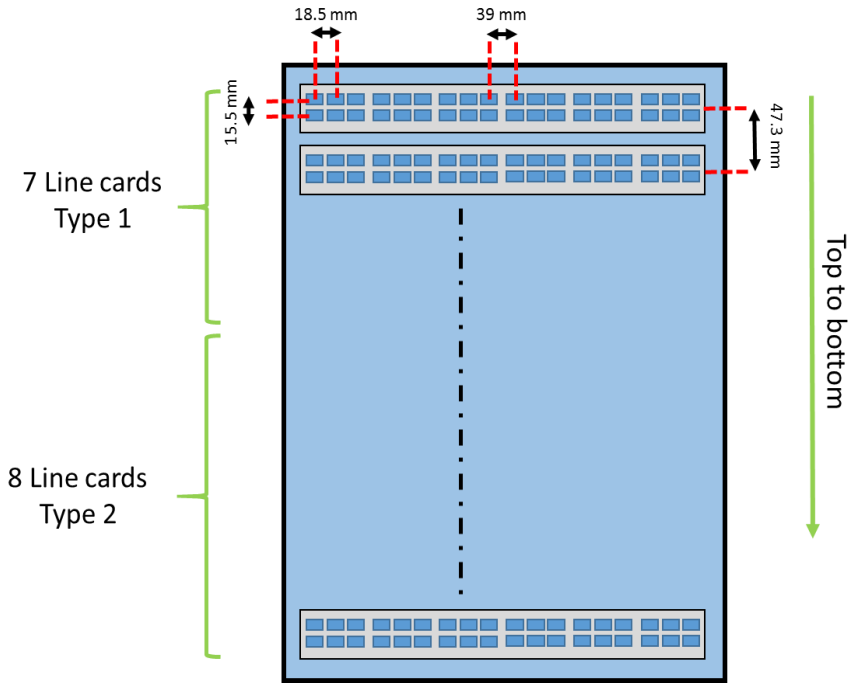

Figure 8.2. Geometrical details of EUT 2 for the array antenna system implementation in the MCS simulation.

As mentioned previously, this study deals with 2 scenarios : first scenario happens when there is just one line card and all the optical modules radiate at exactly the same frequency. This whole structure forms one array antenna with same emission frequency. Second scenario happens when there are multiple line cards in a system and their radiating frequency is slightly off from each other but individual line cards have same frequency. This whole structure forms multiple array antenna with different frequency of

emission. The structural outline in Figure 8.3 provides the implementation of these two scenarios in our MCS simulation along with the input parameters.

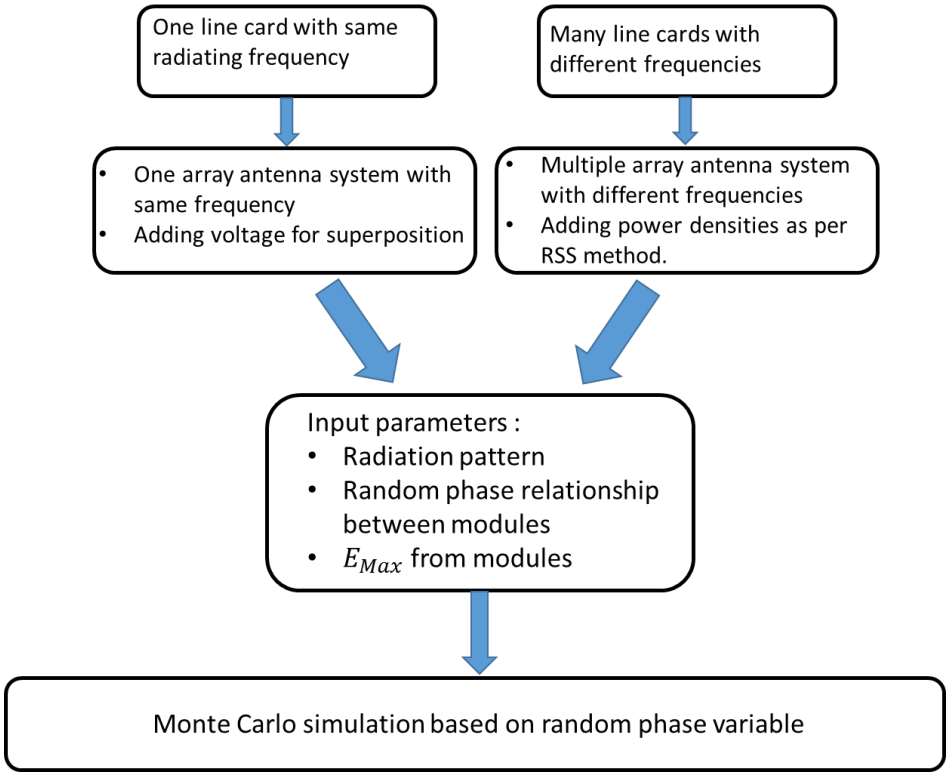

Figure 8.3. Implementation of antenna array theory and MCS simulation for the two scenarios of same frequency and different frequencies under study.

8.2 MONTE CARLO SIMULATION RESULTS AND COMPARISON WITH MEASUREMENT DATA

The total E field strength from a fully populated system was calculated using the simulation. The simulation was ran 1000 times, each time the phase variable was randomly distributed among each elements. The result for E_{Max} based on the number of

iteration for randomly distributed phase variable is shown in Figure 8.4. It states that in a very rare case, the E_{Max} will be higher than 62.5 dBµV/m.

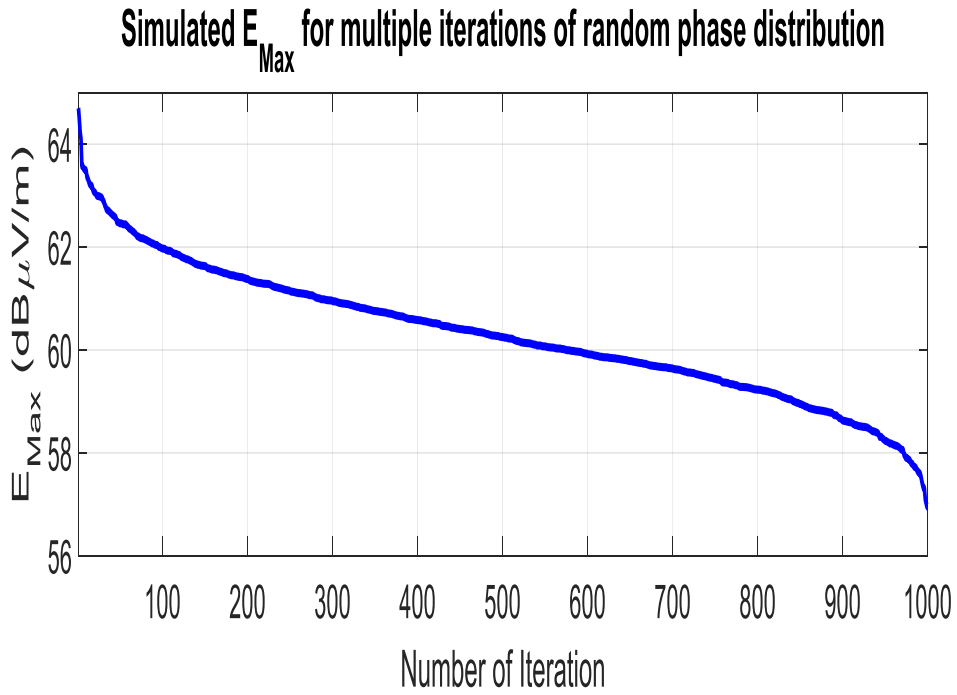

Figure 8.4. Simulated E_{Max} for 1000 iterations for a planar array antenna with random phase excitation.

Now, by means of the MCS and counting the number of occurrences for each E_{Max} in the total iterations, one can find the probability of possible E_{Max} from a fully loaded system. Here CDF is applied to represent the probability of occurrences. The CDF result is shown in Figure 8.5 for 1000 times iteration for E_{Max} with random phase distribution. For example, there is a chance of 95% that the E_{Max} from a fully loaded system with EUT 2 specifications will have a value of 62.5 dBµV/m or less.

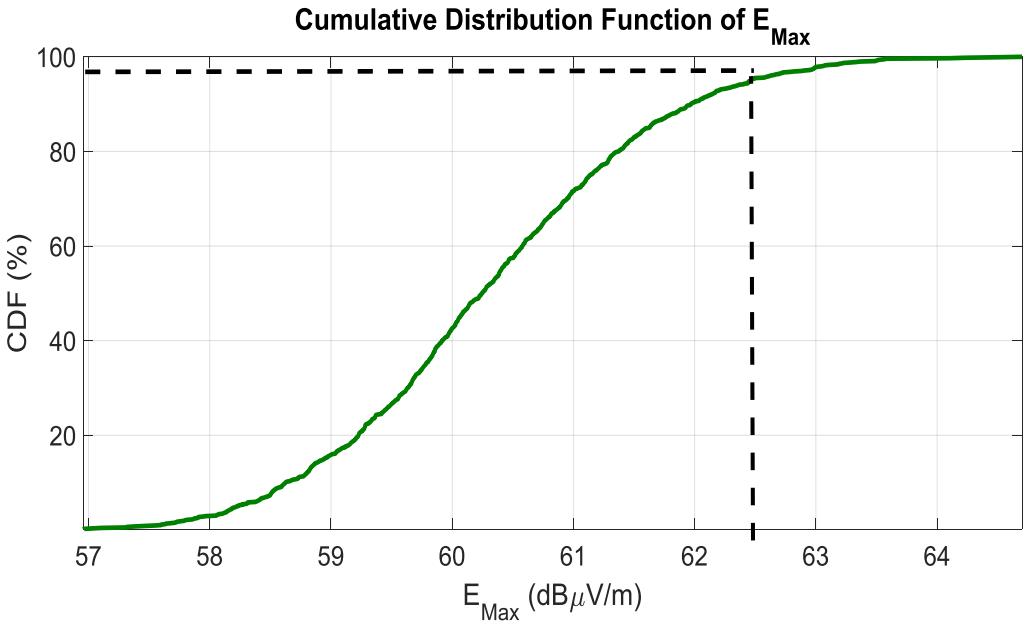

Figure 8.5. Cumulative Density Function (CDF) for E_{Max} from a planar array antenna as per EUT 2 geometry.

The corresponding E_{Max} simulation associated with the 50% chance of occurrence was compared to the measurement results which is illustrated in Figure 8.6. Both the cases were addressed in this comparison including the same frequency for all line cards which led to adding voltages, and different frequency per line card which led to adding power and averaging on it. The measurement was performed on EUT 2 with 15 line cards and receiving antenna at a distance of 3 m. From the comparison of the case for different frequencies where we add power as superposition of increasing number of elements, it is evident that the measurement results and the simulation results are in close agreement with each other. But from the slope of the curve, when multiple radiators are present in a system and all of them are radiating at the same frequency, a growth pattern of *10log N* tendency can be derived where *N* is the number of radiating elements.

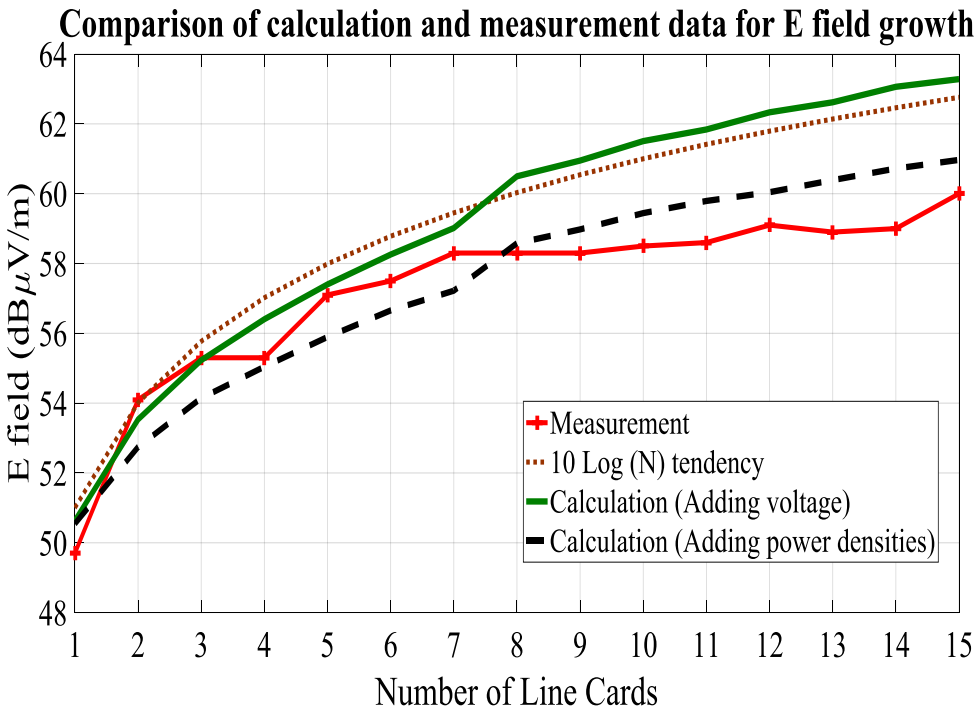

Figure 8.6. E_{Max} growth comparison with incremental number of line cards for numerically simulated results for 50 % chance of occurrence as per CDF results.

It seems the tendency of E_{Max} growth is same as the tendency of TRP growth, at least it is the case when all the line cards are radiating at the same frequency. However, as the measurement was performed on a system with multiple line cards radiating at slightly different frequencies, the growth doesn't match and is less than the *10log N* tendency. In order to validate this result, TRP measurement of EUT 2 was performed in a reverberation chamber. Figure 8.7 shows the actual photo of EUT 2 TRP measurement inside a reverberation chamber and Figure 8.8 shows the results of TRP measurements for various cases of incremental hardware population in EUT 2.

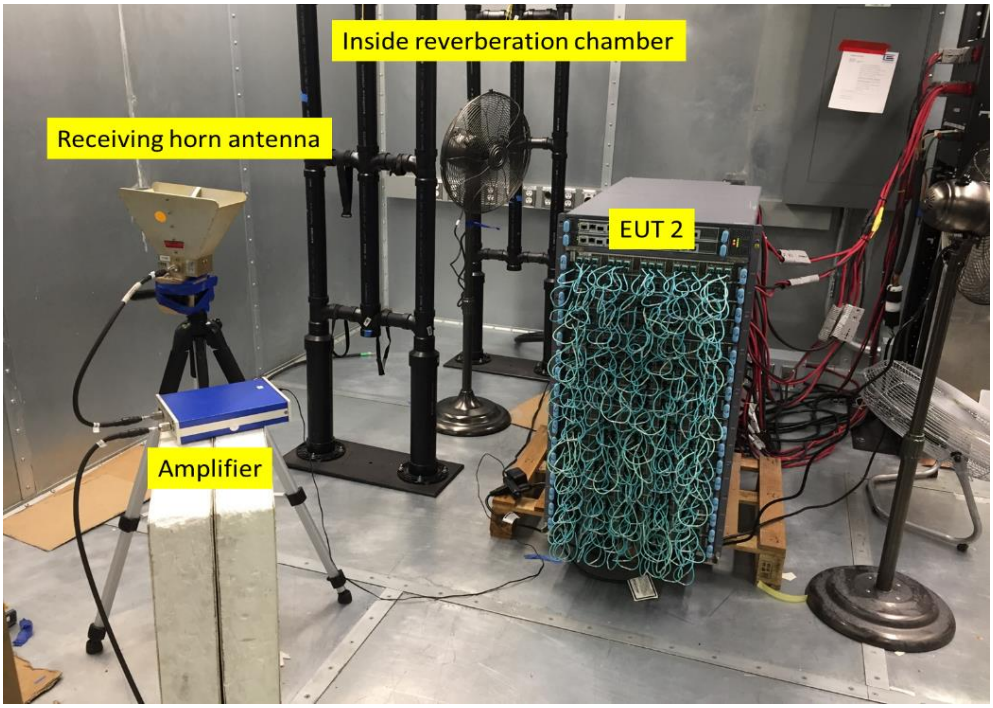

Figure 8.7. Actual photo of EUT 2 inside a reverberation chamber for TRP measurement.

This measurement was carried out with each line card populated into the EUT 2 and the total radiated power was recorded for every hardware addition with 200 times averaging. The receiver settings were kept same as E_{Max} measurement in a 3 m semi-anechoic chamber.

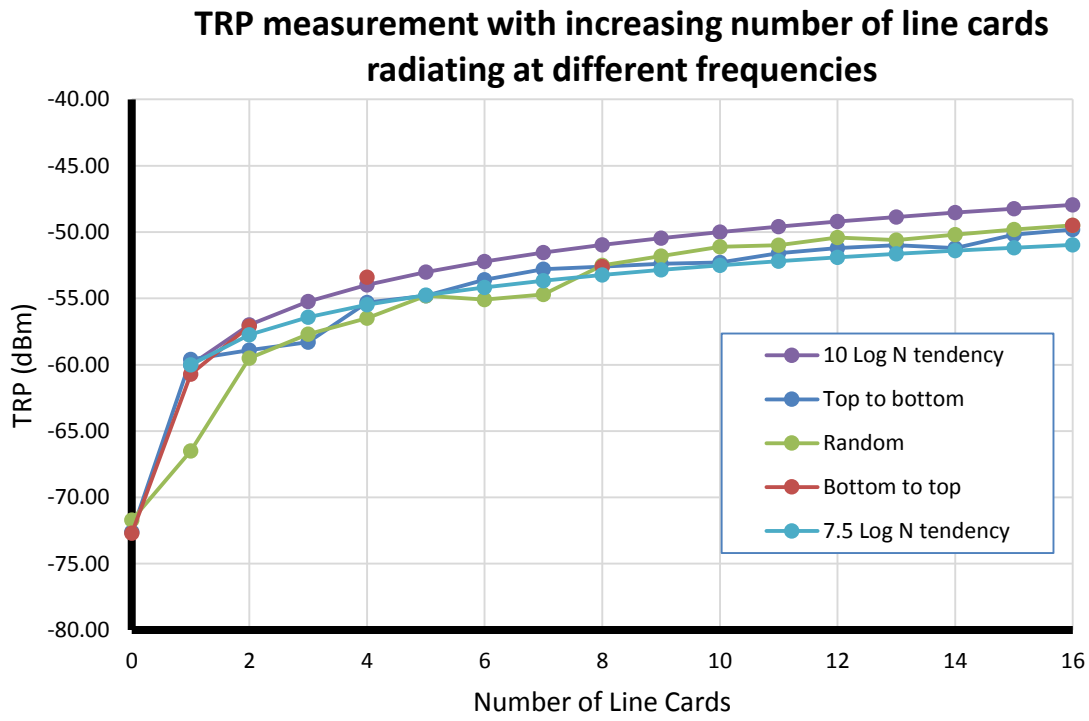

Figure 8.8. Results from the TRP measurement of EUT. Each curve represents a unique sequence of hardware population. Top to bottom and bottom to top represents the cases when the line cards are populated from top slot to bottom slot and again from bottom to top slot respectively in sequence. Random curve represents the growth of TRP when line cards are populated in a random sequence into the slots.

The legend description in the plot is as below:

Legend	Description
10 log N tendency	Simulated curve showing the 10 log N growth tendency starting with the same initial value of measured TRP.
Top to bottom	The line cards were populated sequentially starting from top slot all the way to bottom slot in EUT 2.
Random	The line cards were populated into the EUT 2 slots randomly.

Bottom to top	The line cards were populated sequentially starting from the bottom slot all the way to the top slot in EUT 2
7.5 log N tendency	Simulated curve showing the 7.5 log N growth tendency with the same starting value of measured TRP.

The E field measurement on EUT 2 for "Top to bottom" case and "Bottom to top" case is shown in Figure 8.9. For curve fitting, the x-axis was converted to log scale (shown in Figure 8.10) and the slope was calculated using:

$$m = \frac{y2 - y1}{x2 - x1} = \frac{58.5 - 49.7}{log10 - log1} = 8.8$$

Thus, applying straight line equation of $y = mx + c$, we get $8.8\log(N) + c$. The constant c is the initial value of the curve with just 1 line card.

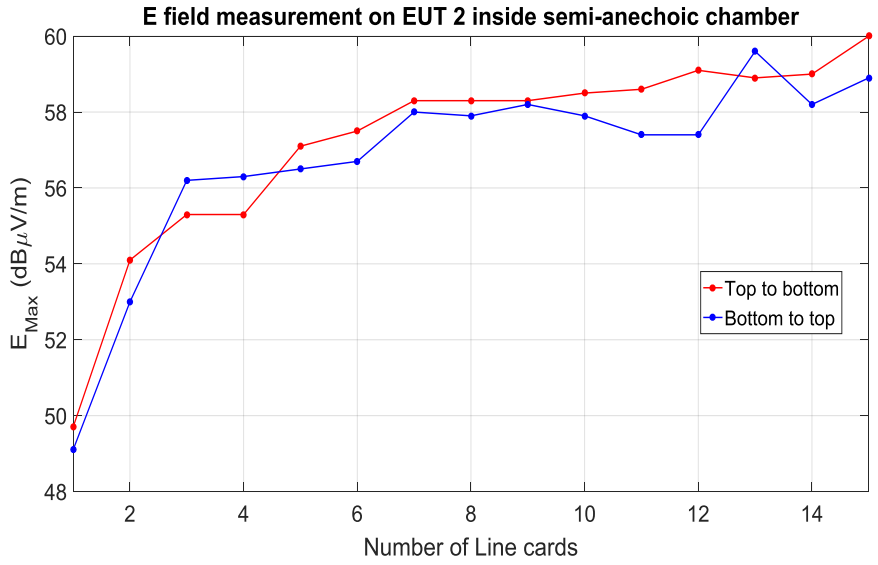

Figure 8.9. E_{Max} measurement inside a semi-anechoic chamber for 3 m distance for two different ways of line card population in EUT 2.

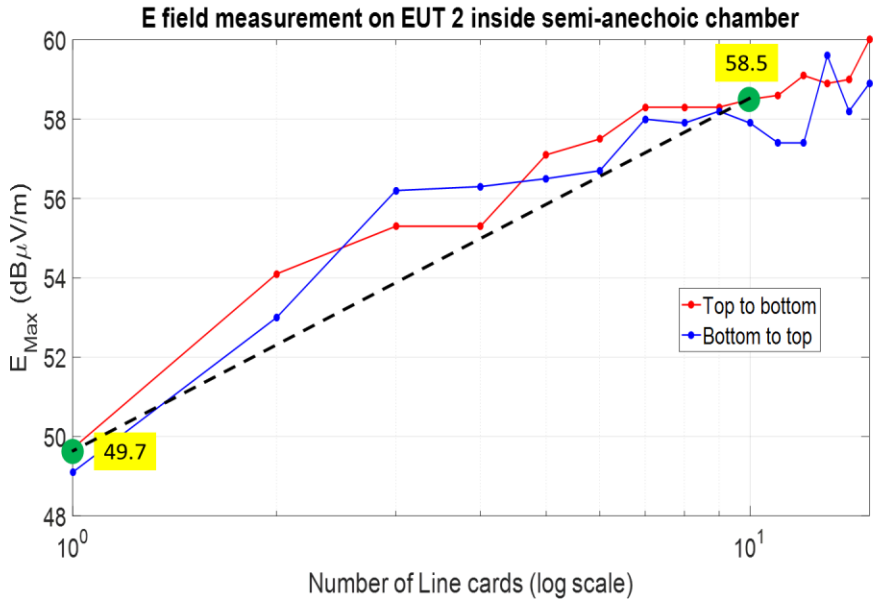

Figure 8.10. E_{Max} curve fitting (logarithmic) to calculate the slope of E field growth pattern.

Thus, the E field curve shows a pattern of *8.8log N* growth tendency. Also, from the TRP curves, it's clearly evident that the growth pattern is less than *10log N* tendency but more than *7.5log N* tendency. Hence, comparing the results of TRP and E field for both the cases of same frequency and different frequencies, the growth of E field from multi-modular system follows the trend of TRP growth.

9. CONCLUSION AND FUTURE WORK

A systematic methodology to estimate the growth of EMI radiation from a large multi-modular system has been studied and validated. The systematic approach refers to identifying the main radiator element in a complex system and evaluating the electromagnetic parameters of the elements for their frequency components, radiation pattern, phase relationship, TRP and E_{Max} data. In any large system, presence of multiple radiators essentially produces an array antenna; however the array system formation will be dependent on the frequency of emission. If all the elements are radiating at same frequency, then it forms on large array antenna system whereas, if they are radiating at different frequencies it may form multiple array antenna system. Accordingly further steps should be taken to implement these parameters and theory to Monte Carlo simulation which handles the random distribution variable very accurately and generate a Cumulative distribution function for E_{Max} . It is very important to understand the radiation pattern, its implication towards the standardized radiated emission measurement setup and hence the directivity because is a key parameters to the relationship between TRP and E_{Max} .

After characterizing the radiating elements electromagnetically, one should perform TRP and E_{Max} measurement with only one element plugged into the system. Once the relationship between them is established, it is confirmed that the identified parameters can be used as the input variables in the statistical simulation. While evaluating radiation pattern, E_{Max} and TRP, extreme care needs to be taken in order to prevent contribution from any other radiating sources which do not multiply with addition of hardware like vents, slots or other mechanical aberrations in the chassis

structure. E_{Max} is calculated from equation (12) with directivity D_{max} from the radiation pattern measurement using equation (11) and TRP (max or average) from one element measured in a reverberation chamber. This E_{Max} is used in the statistical simulation input along with phase information and radiation pattern data. Based on the frequency of radiation from the sources, superposition of voltage (same frequency) or power is applied in the Monte Carlo simulation. The output of the Monte Carlo simulation is chosen as CDF due to its ability to represent the E_{Max} values in a more comprehensible manner. Thus, it was shown that depending on the chances of occurrences, an extrapolation of E_{Max} can be obtained for the total number of designated modules in the system. It can also be concluded that the growth of E_{Max} follows the growth tendency of TRP (based on voltage superposition or power superposition). Thus, measured TRP data from fewer hardware can also be used in the growth tendency curve (lies between *7.5 log N and 10 log N)* to extrapolate curves for E_{Max}. The constant *'c'* in the curve defines the starting level of E_{Max}.

The major advantage of this methodology is the cost of hardware and testing time can be reduced significantly. For manufacturers of large complex system, this methodology will prove to be very useful as based on the results from this algorithm a calculated risk can be taken towards the improvement of design, replacement of hardware and prototype manufacturing. The approach in this study is implemented and verified using a real complex system of network switch which holds 16 line cards and a total of around 500 optical transceiver modules (main radiating element). The simulation results and measurement results are in close agreement with each other within measurement uncertainties. The cause of deviation and standard E_{Max} measurement process related

imperfections can be continued as future work. As for EMC, the contribution from mechanical and structural artifacts is imperative, investigating on the degree of deviation from various module manufacturer designs, grounding and shielding strategies can also be included as future work on this topic.

10. FLOW DIAGRAM OF THE METHODOLOGY

A flow diagram of this methodology is shown in Figure 10.1:

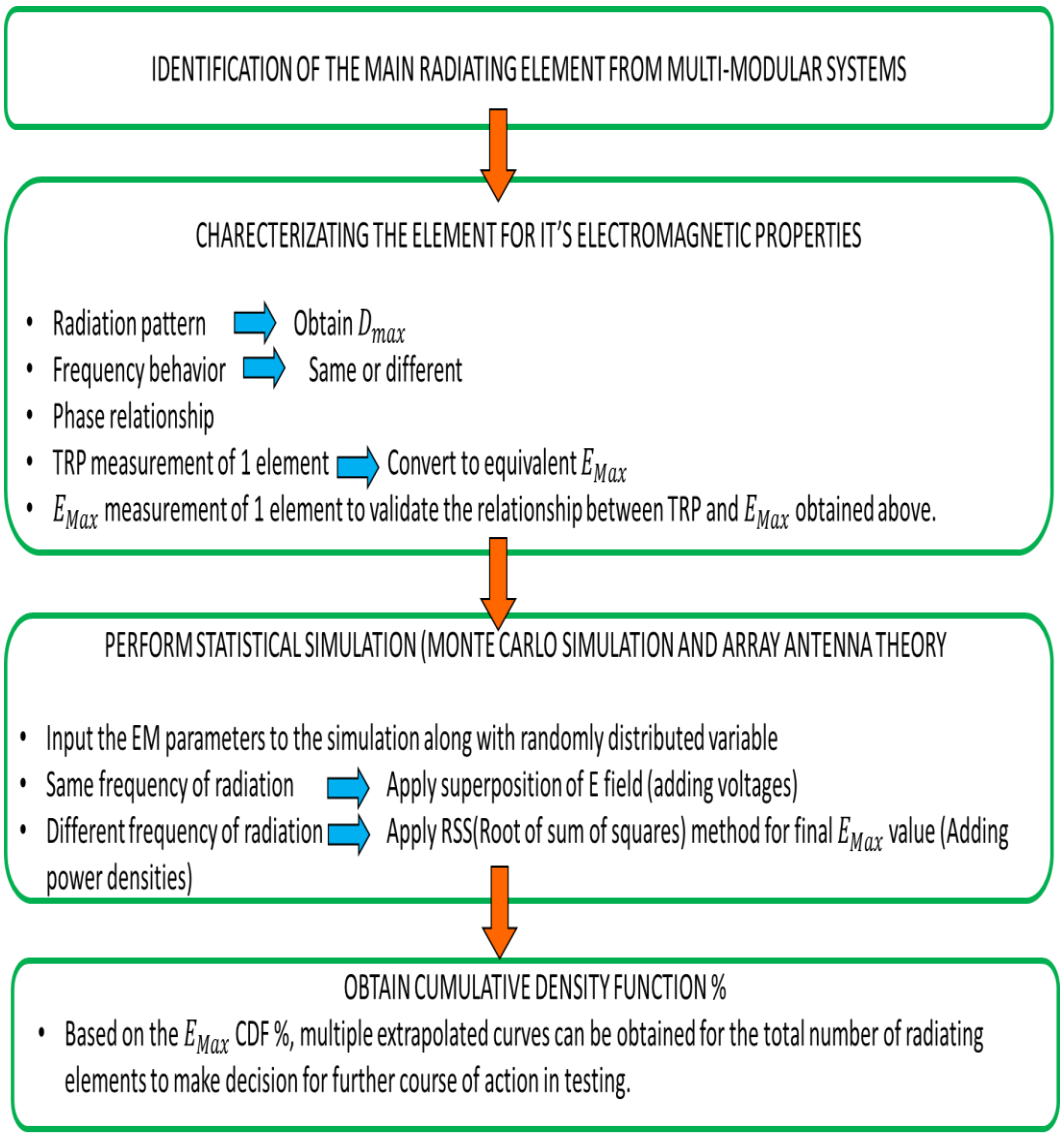

Figure 10.1. A flow chart of the EMI Scaling methodology based on MCS and array antenna theory

RSS method : $E_{Max} = \sqrt{(E_1)^2 + (E_2)^2 + \cdots + (E_n)^2}$

Where, E_1, E_2 ... E_n corresponds to individual sources in the system.

Alternative path for quick estimation is shown in Figure 10.2:

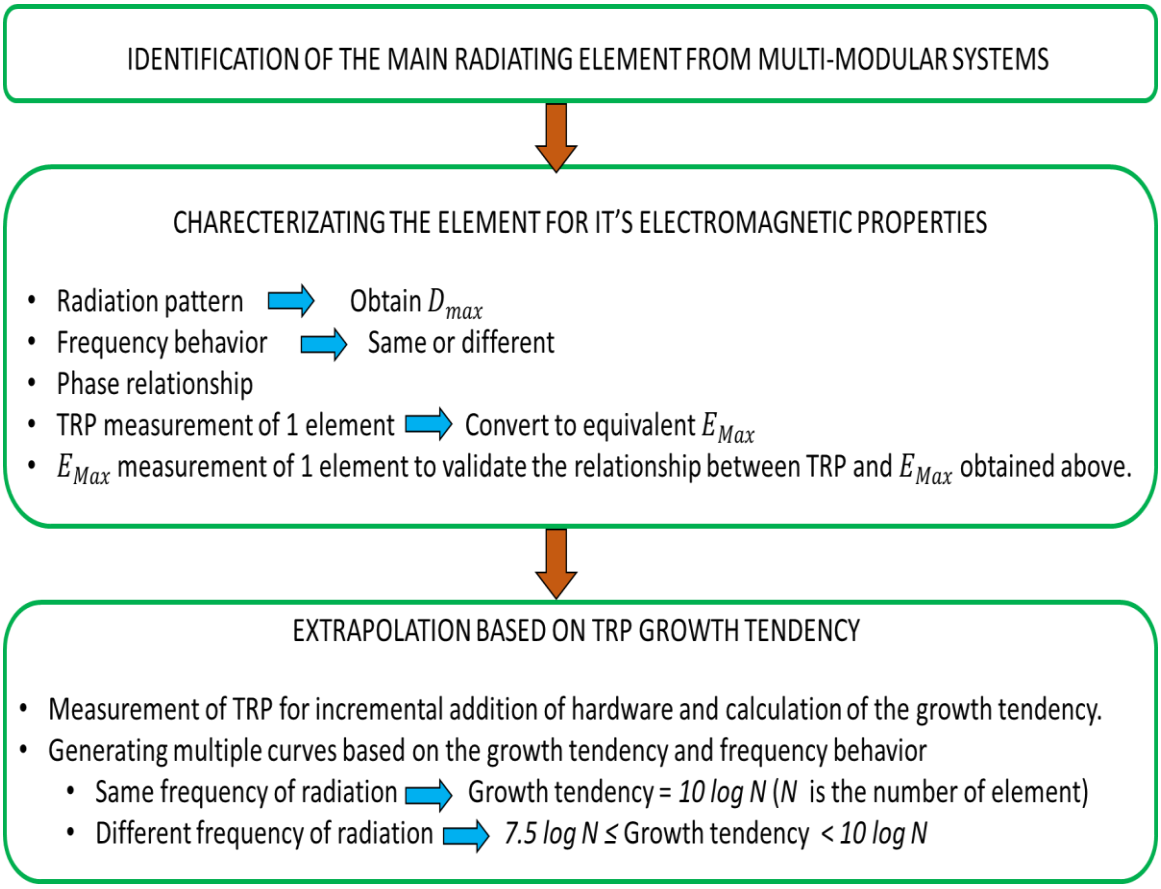

Figure 10.2. A flow chart of an alternate path in the scaling methodology based on TRP growth tendency.

BIBLIOGRAPHY

[1] J. Hansen, “Spherical Near-Field Antenna measurements”, London: Peter Peregrinus Ltd., 1988.

[2] B. Menssen, D. Hamann, H. Garbe, “Predicting the maximum radiated electric field strength from unintentional radiators”, 2015 Asia-Pacific Symposium on Electromagnetic Compatibility (APEMC), pp. 456-459

[3] G.Koepke, D.Hill and J.Ladbury, “Directivity of test device in EMC measurements”, IEEE International Symposium on Electromagnetic Compatibility, vol 2, 2000, pp. 535-539.

[4] Xiaowei Wang and Ralf Vick, "Directivity and Effective Radius of an Electrically Large EUT with Attached Wires", Otto-von-Guericke-University, Magdeburg, Germany

[5] C.L. Holloway, P.F. Wilson, G.Koepke, M.Candidi, “Total radiated power limits for emission measurements in a reverberation chamber”, 2003 IEEE International Symposium on Electromagnetic Compatibility, vol.2, pp. no. 838-834.

[6] H. Garbe and S. Battermann, “ Converting total radiated power measurements to equivalent E-field data”, Aug 2008, pp. 1-6

[7] P.F. Wilson, D.A. Hill, C.L. Holloway, “On determining the maximum emission from electrically large sources”, 2002 IEEE Transactions on Electromagnetic Compatibility, vol 44, pp.79-86.

[8] G. Wong, B. Livshits, ”Extrapolation of Emanations from Large Systems”, 1994 International Symposium on EMC, Sendai Japan, pp 253-255

[9] J.LI, S.Toor, A.Bhobe, J.L.Drewniak, J.Fan, “Radiation physics and EMI coupling path determination for optical links”, 2014 IEEE International symposium on electromagnetic compatibility (EMC), pp. 576-581

[10] Constantine Balanis, Antenna Theory- Analysis and Design, 3rd edition by Wiley and sons, May 2005

[11] J.Li, X.Li, X. Jiao, S.Toor, L.Zhang, A.Bhobe, J.L.Drewniak, D. Pommerenke, “EMI coupling paths in silicon optical sub-assembly package”, 2016 IEEE International symposium on electromagnetic compatibility (EMC), pp. 890-895

[12] H. G. Krauthäuser, Grundlagen und Anwendungen von Modenverwirbelungskammern, 1st ed., ser. Res Electricae Magdeburgenses, Magdeburger Forum zur Elektrotechnik. Magdeburg: Nitsch, Jürgen and Styczynski, Zbigniew Antoni, Jan. 2007, no. 17.

[13] R. Billinton and W. Li, “Reliability Assessment of Electric Power Systems Using Monte Carlo Methods”, New York: Plenum, 1994.

[14] Electromagnetic Compatibility (EMC) - Part 4-21: Testing and Measurement Techniques - Reverberation Chamber Test Methods, IEC 61000-4-21, 2011.

[15] http://www.antenna-theory.com/definitions/trp.php. September 2017.

VITA

Kaustav Ghosh earned his Bachelors degree in Electronics and Telecommunication Engineering from Priyadarshini College of Engineering, Nagpur University, India in 2012. After completion of his bachelors degree, he worked as a Systems Engineer at Infosys Ltd, Pune, India for 2.5 Years (till June 2015). He has been a graduate student in the Electrical Engineering Department at Missouri University of Science and Technology since August 2015 and worked as a Graduate Research assistant under Dr. David Pommerenke from April 2016 to August 2018. He received his Masters degree in Electrical Engineering from Missouri University of Science and Technology in December 2018.